UNIVERSITY
INSTITUTE
OF LISBON

Remote Sensing for Catastrophic Scenarios - LiDAR Data from Project Agile

Lídia Mariana Lourenço Marques

Master in Computer Science and Business Management

Supervisor:
PhD Octavian Adrian Postolache, Full Professor,
Iscte – Instituto Universitário de Lisboa

Supervisor:
PhD Mariana Catela Jacob Rodrigues, Assistant Professor,
Iscte – Instituto Universitário de Lisboa

October, 2025

TECHNOLOGY
AND ARCHITECTURE

Department of Information Science and Technology

Remote Sensing for Catastrophic Scenarios - LiDAR Data from Project Agile

Lídia Mariana Lourenço Marques

Master in Computer Science and Business Management

Supervisor:
PhD Octavian Adrian Postolache, Full Professor,
Iscte – Instituto Universitário de Lisboa

Supervisor:
PhD Mariana Catela Jacob Rodrigues, Assistant Professor,
Iscte – Instituto Universitário de Lisboa

October, 2025

Acknowledgments

First, I would like to thank my parents for everything they have done for me, not only this past year in helping me complete my thesis, but throughout all the years before. Without a doubt, they have always been the first to believe in me, and for that, I am eternally grateful.

I would also like to thank my second family, the Bombeiros Voluntários de Vila de Rei. During the trips between home and the fire station, they supported me throughout this challenging journey, and I am deeply grateful to them as well.

I would also like to thank my godparents for supporting me during the first year of my master's degree. You too are a reason for this success.

Finally, I would like to thank my two supervisors, Octavian Postolache and Mariana Rodrigues. Without your guidance, I would never have found the best way to achieve my thesis goals.

It has been an incredible and tough journey, but I have never walked alone.

To all of you, thank you very much.

Resumo

LiDAR é uma tecnologia de teledeteção ativa (também conhecida como sensoriamento remoto) que mede a distância de um alvo e recolhe dados espaciais desse objeto utilizando feixes de laser emitidos por um sensor optoeletrónico. Os dados LiDAR permitem extrair com elevada precisão informações verticais dos povoamentos florestais, apresentando vantagens significativas face à teledeteção ótica passiva convencional. Neste trabalho será analisado o caso do projeto Agile, cujo objetivo é gerar produtos cartográficos a partir de dados de sensores LiDAR aerotransportados, de forma a apoiar a gestão de incêndios florestais e rurais. Para além disso, será abordada a problemática das cheias. O objetivo desta investigação é avaliar o potencial dos dados LiDAR na identificação de áreas de risco, no apoio à tomada de decisão e na melhoria de estratégias de mitigação em cenários de catástrofe.

Palavras-Chave: Remote Sensing; LiDAR; Projeto Ágil; Cenários Catastróficos; Tomada de Decisão.

Abstract

LiDAR is an active remote sensing technology that measures the distance to a target and collects spatial data about it, using laser light emitted by an optoelectronic sensor device. LiDAR data can accurately extract vertical information from forest stands, compared to conventional passive optical remote sensing, and this feature offers unparalleled benefits in forestry applications. In this study, we will examine the Agile project, which aims to generate cartographic products from airborne LiDAR sensor data to support forest and rural fire management. In addition, we will address the topic of floods. The aim of this research will be to investigate the potential of LiDAR data to identify risk areas, support decision-making and improve mitigation strategies in disaster scenarios.

Keywords: Remote Sensing; LiDAR; Agile Project; Catastrophic Scenarios; Decision-Making.

Index

Content

List of Figures

List of Tables

List of Acronymous

RS- Remote Sensing

LiDAR - Light Detection and Ranging

ALS-Airbone Laser Scanning

IPMA- Instituto Português do Mar e da Atmosfera

API- Application Programming Interface

GIS- Geographic Information System

PDR-Post Disaster reconstruction

DTM- Digital Terrain Models

DSM- Digital Surface Model

NAIP- National Agricultural Imagery Program

MPLNET -Micro-Pulse Lidar Network

MPL-micro-pulse lidar

GIT-Geospatial Information Technologies

AQI-Air Quality Index

OGC -Open Geospatial Consortium

ESRI- Environmental Systems Research Institute

ICNF -Instituto da Conservação da Natureza e das Florestas

AGIF -Agência para a Gestão Integrada de Fogos Rurais

DSS- Decision Support Systems

ECMWF- European Centre for Medium-Range Weather Forecasts

APS-Average Point Spacing

TWI- Topographic Wetness Index

CAOP -Carta Administrativa Oficial de Portugal

DGT- Direção Geral do Território

FWI- Fire Weather Index

CEMS / EMS-Copernicus Emergency Management Service

RCM- Índice Conjuntural e Meteorológico

List of Equations

1-Introduction

Remote sensing has become an indispensable technique for monitoring and assessing natural hazards, providing critical information for disaster risk management. Critical information is provided by satellite flood mapping, particularly in areas with limited data, where conventional ground observations are often unavailable or insufficient. By improving the accuracy of hydrological models and facilitating flood vulnerability mapping, the integration of remote sensing with Geographic Information Systems (GIS) provides a solid foundation for disaster resilience and urban planning [1].

Widespread economic losses around the global have been a destructive result of natural disasters, including floods that impact particularly on the coastal areas of European Mediterranean. Increased frequency and intensity of extreme precipitation events in the last few decades, have made flooding more severe especially in urban areas with high concentrations of inhabitants. In the western Mediterranean area, cut off low pressure clouds frequently lead to very moist surface conditions and heavy autumnal rainfall, which are optimal for wide-spread flooding [1].

Other natural disasters such as forest fires are a growing environmental concern due to population growth, urbanization, and human activities, contributing to climate change. They destroy vegetation, habitats, soil, and release toxic gases into the atmosphere, threatening the lives of inhabitants. Remote sensing (RS) is widely used for monitoring and early detection of environmental hazards, while ground-based data are used to investigate forest fires and air quality assessments [2].

Not only remote sensing techniques, but also the analysis of observational climate data can help characterize flood development and perform a flood risk assessment to identify risk areas useful in developing policies against flood events. Satellite images can be used to identify flooded areas, while precipitation and soil moisture anomalies and heavy rainfall trends can be analysed using climatological data [3]. In addition, remote sensing data, including satellite platforms such as Sentinel-1 and Sentinel-2, and meteorological data from NASA Power and the European Centre for Medium-Range Weather Forecasts (ECMWF), can be leveraged to develop machine learning and deep learning models for estimating the severity of forest fires.

The present thesis investigates the role of remote sensing in catastrophic scenarios, highlighting its significance for disaster assessment and management [4].

1.1. General Objectives and Motivation

In recent decades, the world has witnessed a significant increase in the frequency and intensity of natural disasters, such as forest fires, floods, and extreme storms. These phenomena, exacerbated by climate change, put human lives, property, and entire ecosystems at risk. Mitigating and preventing these events requires effective monitoring and forecasting mechanisms capable of providing reliable and timely information to crisis management authorities [5] .

In this context, remote sensing plays a central role. Technologies such as LiDAR (Light Detection and Ranging) enable high spatial resolution measurements to be obtained, capable of describing the morphology of the terrain with great precision. When combined with high-quality meteorological data (such as that provided by the Portuguese Institute of the Sea and the Atmosphere (IPMA)) these measurements can offer an integrated view of risk conditions, enable the mapping of vulnerable areas and support strategic decisions [6], [7].

As demonstrated in various fields of knowledge, from archaeology to environmental management, the multidisciplinary integration of quantitative spatial, morphological, and climatic data allows us to reconstruct complex scenarios and better understand the dynamics of natural phenomena. By applying this approach to the field of disaster management, the goal is to develop solutions that not only monitor but also anticipate potential hazardous events [8].

This work aims to support the decision-making processes of organizations involved in disaster prevention and response by applying advanced geospatial analysis and visualization tools.

The Agile Project is a national initiative aimed at acquiring and providing high-resolution LiDAR data to support land management, risk assessment, and environmental studies. Its database offers detailed topographic information, which is particularly valuable for applications in disaster prevention and response.

By exploring the combination of LiDAR data from the Agile Project with meteorological data from IPMA APIs, the goal is to create an interactive application in Experience

Builder (from ArcGIS Online) that allows the competent authorities to access, interpret, and use this information in a simple, fast, and effective way.

1.2. Methodological Approach (overview)

The methodology adopted in this work is organized into distinct stages, as illustrated in Figure 1.

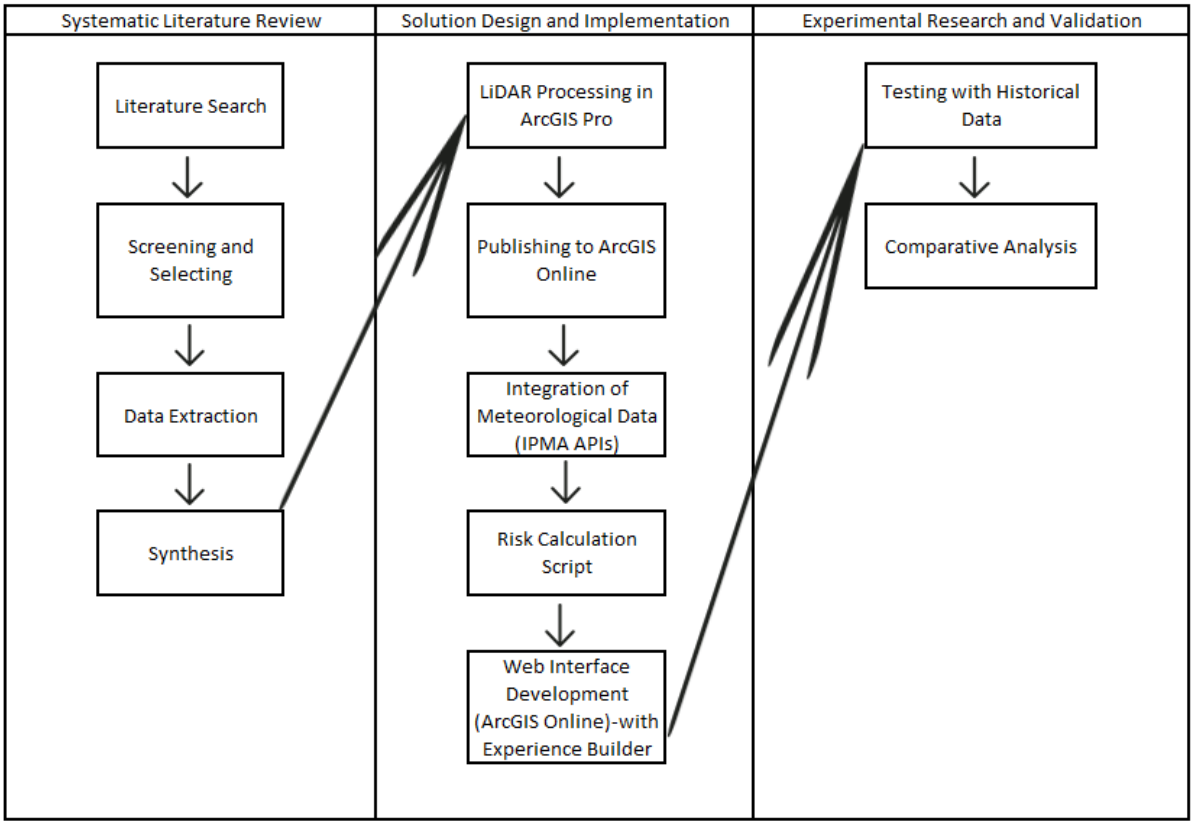

Figure 1-Methodological Approach (overview)

The first phase consists of a systematic review of the literature, including the research, selection, extraction, and synthesis of relevant studies, which provide the theoretical basis for the solution. The second phase focuses on the design and implementation of the solution, involving the processing of LiDAR data in ArcGIS Pro, the integration of meteorological data from IPMA APIs, and the development of a risk calculation script and web interface in ArcGIS Online. Finally, the third phase corresponds to experimental investigation and validation, where the solution is tested with historical data and subjected to a comparative analysis to assess its accuracy and effectiveness.

1.3. Research Questions and Hypotheses

The research focuses on the following questions:

RQ1: Can we use a combination of remote sensing data, such as LiDAR data from the Agile Project, to accurately predict the risk of fire and flooding in the project area?

RQ2: Can ArcGIS Experience Builder be used to integrate LiDAR data from the Agile Project with IPMA APIs through Python scripts?

1.4. Document Structure

This document presents the development of a disaster management App that integrates LiDAR data with meteorological information used by IPMA.
Chapter 1 presents the project, providing the motivation, general aims, research questions, and hypotheses underpinning the research. Chapter 2 establishes the Literature Review, giving the theory context as it presents disaster management issues and challenges, LiDAR technology principles and applications, the significance of meteorological data sources such as IPMA and their APIs, and the use of Geographic Information Systems: ArcGIS Pro, ArcGIS Online, and QGIS. Chapter 3 provides a description of the Methodology, determining the sources of data, their treatment and preparation, and defining parameters for risk assessment. Chapter 4 describes the Application Development phase, detailing the system architecture, LiDAR data processing workflow, meteorological data integration procedures, risk calculation algorithm design, and web interface development using Experience Builder (ArcGIS Online). Chapter 5 presents the Results and Discussion, including the application demonstration, validation using historical events, and comparative analysis with existing tools and methodologies. Chapter 6 is the Conclusions, with the main contributions, limitations and future work. The Appendices englobe the application link.

2. Literature Review

2.1. Disaster Management: Concepts and Challenges

Figure 2 refers to the disaster management cycle, whose components will be discussed in more detail throughout this chapter:

Figure 2-Disaster Management Cycle[8]

Disasters cause extensive losses of human lives and property, and big disasters are bound to occur more frequently due to reasons such as uncontrolled urbanization, environmental pollution, pandemics, and climate change. Disaster management systems must perform their functions effectively to counteract damage [9].

Disasters are sudden events that disrupt everyday life and result in physical, economic, and social losses. The 21st century has been considered the "century of disasters" because calamities and tragedies have become more frequent. People experiencing disasters are likely to develop physical, cognitive, economic, psychological, and behavioural problems, which take a long time to heal from and can even turn into chronic mental illnesses [10].

Disaster management is divided into four phases: preparedness, response, recovery, and mitigation [9].

"Preparedness enhances readiness for all hazards. Preparedness entails continuous planning, organization, training, and equipping to enhance readiness to respond to all hazards, incidents, and emergencies. Activities include developing mutual aid agreements, conducting disaster exercises, and conducting all-hazards education campaigns" [11].

For example, preparedness for disasters is fundamental to psychiatric nurses as it reduces the risk of having negative life experiences. The International Council of Nurses places particular significance on skills and knowledge in managing disasters. The research showed that those with theoretical and practical preparation perceived disaster preparedness more. The more experienced and educated head nurses valued disaster preparedness more. Professional training in disaster management, years of working experience, and age also have significant contributions toward disaster preparedness, and disasters can traumatize individuals and society, hence it is necessary that psychiatric nurses be prepared and respond to them [10].

Rapid response saves lives and minimizes losses. The response phase in the immediate period following a disaster encompasses measures to minimize financial loss, save lives, and reduce suffering. Mobilization of resources, setting up emergency operation centers, evacuation of at-risk population, and provision of basic services such as shelter and medical care are among the steps [11].

To mitigate the effects of disasters, health care is important, and nurses have an important role to ensure affected individuals receive appropriate care. Professional commitment, patriotism, spirituality, safety, family obligations, protective equipment, health, and transport matters are some of the determinants of the willingness of nurses to work in emergencies. Another important factor that can influence nurses' willingness to work in emergencies is self-efficacy. According to research, self-efficacious nurses are willing to engage in actions in risky and uncertain emergency situations [12].

Once the immediate threat to human life has passed, recovery activities begin, with an emphasis on minimizing long-term damage and restoring essential community services. Activities include debris removal, financial assistance, infrastructure restoration, and ongoing support for displaced persons until everything returns to normal [11].

Post-disaster reconstruction (PDR) following natural and man-made disasters is a challenging process, with global disasters claiming around 1.23 million lives over the past two decades.

Reconstruction activities are influenced by many factors, such as the political environment, management of a project, stakeholders, technological challenges, finances, and social elements. Recent studies have broadened the understanding of issues arising after disasters, with the incorporation of technology and newer structures [13].

The Yemen case, for example, illustrates how natural disasters and war, including floods, earthquakes, and ongoing wars, have further worsened an already severe humanitarian

crisis. Barriers to Yemen's rebuilding are multi-dimensional, from political turmoil to economic constraints, human resource deficiencies, ongoing war, and so on. Additionally, Yemen is under threat of massive rebuilding by disasters of natural and man-made origin supplemented by poor finances, ineffective governance, bureaucratic inclinations in institutions, corruption, and coordination failures. Overcoming these issues requires early identification and understanding of the primary drivers affecting rebuilding. It is crucial to set project priorities against aims and assess their impact. Effective project management is required to address these problems and seize chances to avoid delays, enhance quality of life, and encourage displaced people to return home. Utilization of the local potential is essential to achieve sustainable recovery and reconstruction in Yemen [13].

Its effects are minimized by mitigation. It encompasses measures of avoiding or diminishing harmful effects. Mitigation programs aim at minimizing the effect of disasters and emergencies, which in turn will decrease loss of property and lives. They comprise enforcing building codes, zoning regulations, and designing defensible zones around homes to protect against wildfires [11].

Sustainable hazard mitigation means conserving and enhancing environmental quality, human quality of life, local responsibility and resilience, recognizing living local economies, inter and intra generational equity promotion, and local consensus building adoption.

Other authors believe that one should complete hazard, risk, and vulnerability analysis before implementing sustainable hazard mitigation and community planning. The interconnection of sustainable hazard mitigation and community planning should be addressed to have an effective disaster management process [14].

In North America, public engagement is increasingly part of the disaster response process, as examples such as the Home Emergency Response Organization System in British Columbia, which involves enlisting leaders and volunteers from each neighbourhood to create a neighbourhood inventory of equipment and skills, develop a list of special-needs circumstances, and coordinate local stockpiling of medical supplies, food, and water. Also, recent studies indicate that disaster management in Australia is moving its concentration from response and recovery concerns to mitigation concerns, which includes an executable space for public involvement [14].

The cycle has a fifth step of disaster management that is called prevention which tries to reduce or eliminate the risks. Though it is not possible to eliminate risk entirely,

precautionary techniques substantially minimize risk of injury and fatality like avoiding risk, whether technologic, natural or anthropogenic [11].

To put this into context, let's take the example of what happened in Portugal in 2017. That year, Portugal faced one of the most devastating forest fire seasons in its history, with more than 117 deaths and around 540,000 hectares destroyed. These events, including the Pedrógão Grande fire in June and the October fires fuelled by Storm Ophelia, highlighted significant flaws in the country's disaster management [15].

Prevention and Mitigation: Prior to 2017, forest management and fire prevention had significant gaps, such as a lack of adequate vegetation management and the extensive presence of highly flammable species. The tragedy highlighted the need for more effective mitigation measures, including restrictions on eucalyptus planting and evidence-based risk management policies [16].

Preparedness: Emergency preparedness proved insufficient, especially in risk communication and evacuation plans. Many residents did not receive adequate warnings, and the resources available were limited to deal with the magnitude of the fire

analysis of these events highlights the need to strengthen training programs, warning systems, and coordinated contingency plans [17].

Response: During the fires, the immediate response encountered logistical and operational challenges. The Pedrógão Grande fire revealed critical problems in coordination between emergency forces, communication failures, and difficulties in evacuating isolated communities. These incidents underscored the importance of an integrated, rapid, and efficient response to reduce human and material losses [18].

Recovery: After the fires, Portugal began recovery and reconstruction efforts, focusing not only on the physical restoration of the affected areas, but also on psychosocial support for communities and strengthening local resilience. This process included legislative reviews, improvements in firefighting infrastructure, and the implementation of more proactive risk management approaches [19].

In conclusion, the management of the 2017 fires marked a turning point for Portugal, catalysing a transformation in its approach to the prevention, preparedness, response, and recovery from natural disasters.

2.2. Remote Sensing Technologies: LiDAR – Principles and Applications

LiDAR is an active remote sensing technology that operates by transmitting laser pulses towards a target and measuring the time that takes for the reflected signal to return to the receiver. This principle, commonly known as time-of-flight measurement, allows for the accurate calculation of distances between the sensor and the object. High precision timing instruments record the duration of the signal's round trip, enabling the creation of detailed three-dimensional representations of surfaces [20], [21].

LiDAR systems can be deployed on airborne, terrestrial, or mobile platforms and have been widely applied in various fields, including the generation of Digital Terrain Models (DTM), 3D reconstruction of urban environments, monitoring of electric transmission lines, coastal mapping, forestry assessment, transportation management, security applications, and cultural heritage studies [22].

In contrast to passive optical sensors, such as those mounted on satellites or aircraft, which rely on reflected sunlight to capture images, LiDAR actively emits its own laser light source [12]. Optical imagery, like that acquired from Landsat satellites or the National Agricultural Imagery Program (NAIP), covers both the visible spectrum (red, green, blue) and non-visible ranges (near-infrared, short-wave infrared, thermal infrared). While optical sensors are highly effective for land cover classification based on spectral signatures, LiDAR provides superior vertical accuracy and penetration capabilities, particularly in vegetated or complex terrain [21].

LiDAR and other remote sensing datasets have proven to be powerful tools for locating archaeological mound sites, as they provide a comprehensive digital overview of the surrounding landscape. Since the 1960s, archaeologists have increasingly adopted remote sensing techniques (beginning with satellite imagery) to identify sites and guide field surveys worldwide. Among the types of sites identified, mound sites are among the most frequently discovered. With the recognition that LiDAR could facilitate archaeological discovery in areas where ground-based survey and large-scale landscape studies are impractical, its application in archaeology has expanded significantly [23].

Airborne LiDAR, also referred to as Airborne Laser Scanning (ALS), is an active remote sensing technology capable of capturing detailed information about the Earth's surface. ALS generates dense, discrete, precise, and detailed 3D point clouds, enabling the direct representation of both objects and terrain. Over the last decade, LiDAR point clouds have

evolved into an essential resource for numerous applications, including the 3D reconstruction of building models [24].

LiDAR is also highly valued in atmospheric research and environmental monitoring due to its fine temporal resolution, high spatial resolution, broad detection range, and ability to perform continuous real time measurements. Unlike in-situ monitoring instruments, which measure only local concentrations, LiDAR can provide large-scale atmospheric observations. The Micro-Pulse Lidar Network (MPLNET), developed by NASA in 1992, exemplifies this capability, using micro-pulse lidar (MPL) to detect aerosols and clouds globally. Advancements in scanning LiDAR have enabled multidimensional atmospheric detection, such as the 1.5 μm scanning LiDAR developed for aerosol monitoring, and systems by Xie et al. for 3D atmospheric detection. In metropolitan areas, LiDAR can map aerosol distribution in the lower atmosphere, contributing valuable information for densely populated regions. The technology's compact size, low weight, and reduced power requirements also enable long term, unsupervised operation [25].

In forestry, LiDAR data can be combined with hyperspectral imagery to enhance species classification. For example, Dalponte et al. (2012) demonstrated that integrating aerial LiDAR with multispectral and hyperspectral datasets improves tree species identification accuracy, especially when tree height data is included. The fusion of hyperspectral and LiDAR data outperformed the use of either data source individually [26].

LiDAR is also applied in biomass estimation, offering a cost effective and efficient approach for assessing bioresources and producing improved spatial resource maps [27].

Within archaeology, LiDAR has emerged as a significant advancement in Geospatial Information Technologies (GIT), enabling non-invasive surveys of sites that may be inaccessible through conventional aerial photography or geophysical techniques [28].

LiDAR measurements can be georeferenced and used to model land surface topography (potentially for 3D GIS mapping) through integration with Global Positioning System (GPS) data via high-precision time synchronization devices [29].

LiDAR technology has been a successful tool in the assessment of wildfire hazards, particularly in nations like Portugal, where wildfires pose a significant danger to natural and urban environments.

By providing high-resolution three-dimensional data on vegetation structure, fuel distribution, and terrain, LiDAR enables researchers to identify high-risk areas and supports strategic decision-making in forest fire management. For example, the authors

of article [30] used LiDAR data to assess the risk of forest fires in the wildland-urban interfaces (WUIs) of central Portugal, revealing that more than half of the territory has high to very high-risk levels, particularly in mountainous areas, thus highlighting priority areas for risk mitigation. Similarly, author from [31] utilized dense pre-fire LiDAR point cloud data in the prediction of fire severity by analysing the vertical pattern of fuel within strata and demonstrated how LiDAR-derived metrics can be utilized to inform pre-fire management and increase preparedness. Complementing these approaches, article [32] integrated LiDAR information with climatological, ecological, and biophysical variables to delimit the riskiest zones to forest fires in Portugal, illustrating how the coupling of LiDAR with other spatial data increases the susceptibility detection to risk-prone areas for specific treatments. Finally, article [33] developed methods to measure apparent fuel density and vertical load distributions directly with airborne LiDAR, providing accurate data on fuel structure, which is important in fire risk estimation and strategic planning. Together, these articles show the potential for LiDAR technology to be used to positive impact in the surveying of at-risk areas, measuring fuel loads, and guiding evidence-based decision making in forest fire risk assessment, warranting its relevance to the context of this thesis.

2.3. Meteorological Data Sources: IPMA and APIs

IPMA is a public institute established by Decree-Law No. 68/2012, supervised by the Ministry of Economy, Agriculture and Fisheries, Education, Science, and Innovation, and Environment and Energy. It aims to maximize the usefulness of public investment by utilizing human and technical resources synergistically. IPMA promotes interaction with various sectors of the economy, including meteorology, climate, fishing, aquaculture, manufacturing, distribution, geology and geophysics. It is committed to international cooperation, focusing on Portuguese-speaking countries, the European Union, and Atlantic countries. The Institute is responsible for providing meteorological services for air navigation, ensuring aeronautical meteorological surveillance and forecasting maintaining national meteorological, geophysical, oceanographic, living resources and fisheries observation networks. It aims to be a leading public institute with high scientific

and technological capacity in meteorology, climate, geophysics, marine geology, marine environment, aquaculture, and marine biotechnology [34].

The IPMA Open Data API is a user-friendly platform that provides rapid access to current meteorological information, including humidity, wind speed, and air quality index (AQI), for any location. These weather API´s are crucial for daily planning and decision-making in industries such as energy, agriculture, and space science. The primary focus of a Weather API is performing, ensuring rapid responses to queries within an acceptable amount of time. To use the API, authentication and authorization are necessary due to financial and commercial reasons. The application's intuitive interface, consisting of HTML, CSS, JavaScript, and Leaflet.js, ensures a lightweight and efficient performance. The Weather API's real-time data updates, user-friendly interface, and lightweight performance make it a valuable tool for anyone seeking a straightforward weather solution. The dedication to data dependability and quality further enhances the usefulness of the Weather API in aiding people in everyday planning and decision-making [35].

The creation of API systems are requirements of European regulations. To comply with these regulations, IPMA has implemented a computer system that allows access to data from meteorological observation systems and climate indicators through international data sharing standards, such as OGC (Open Geospatial Consortium) services and API systems [34].

2.4. Geographic Information Systems (GIS): ArcGIS Pro, ArcGIS Online and QGIS

ArcGIS is a comprehensive GIS software system developed by Environmental Systems Research Institute (ESRI), which offers a wide range of functionality for building operational GIS. The system comprises four key components: a geographic information model, elements for managing and storing geographic data in databases and files, off-the-shelf applications for generating, modifying, modifying, mapping, analysing, and sharing geographic data, and a group of web services that offer capabilities and content to software clients that are networked (Figure 3) [36].

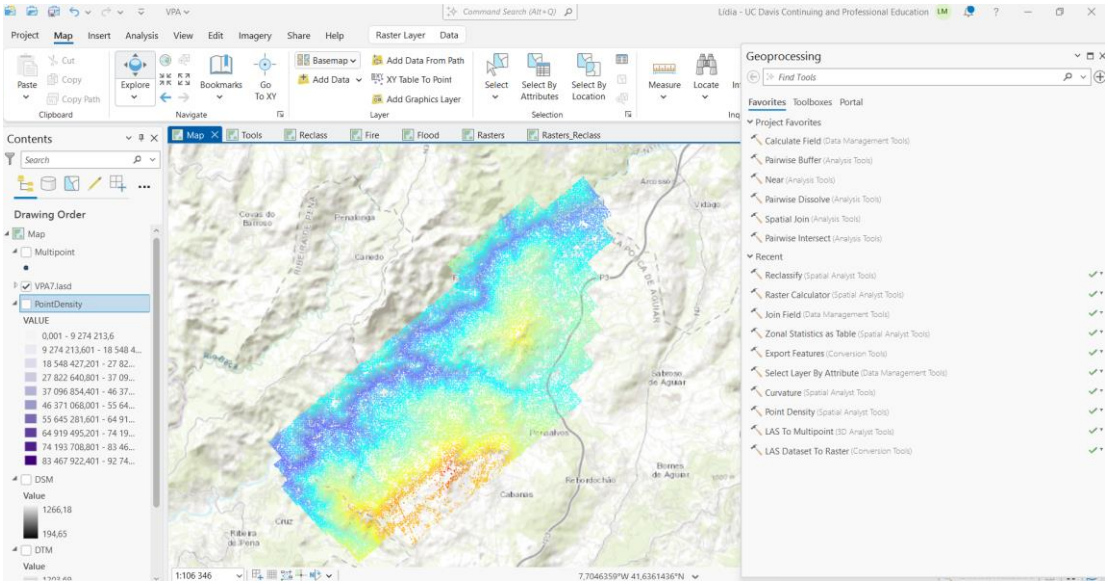

Figure 3-ArcGis Pro Interface

ArcGIS Online provides a set of web services accessible from any web-enabled device, browser, or other application. It is also a developer-friendly product, accessible using various programming paradigms, including within application scripting, web services end points, and component interfaces. Developers can personalize and customize existing software applications, build new applications, embed parts of ArcGIS in other software, and interface with other software systems (Figure 4) [36].

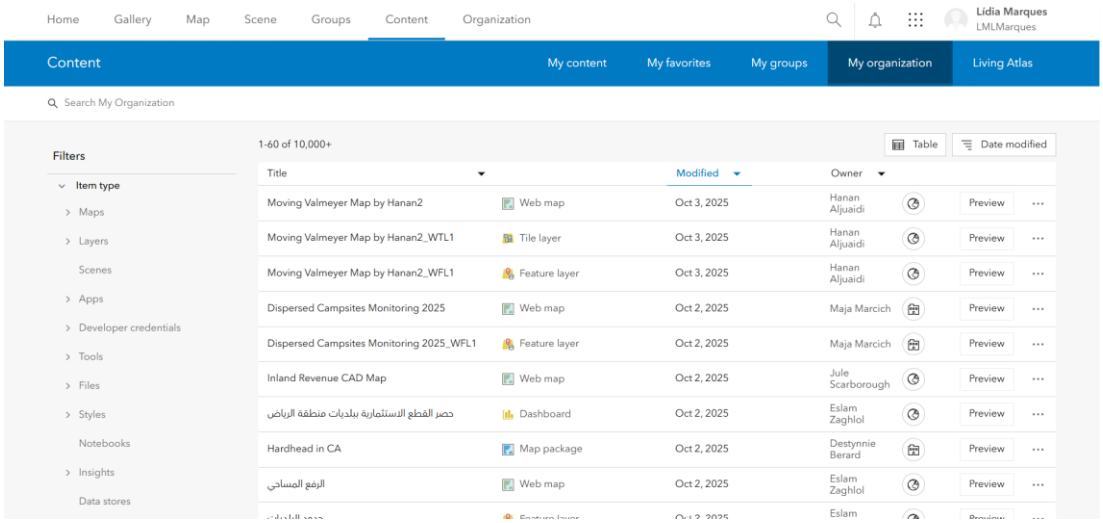

Figure 4-ArcGIS Online Interface

Experience Builder is a web GIS tool that allows users to create desktop and mobile apps in a dash-board fashion. (Figure 5) [37].

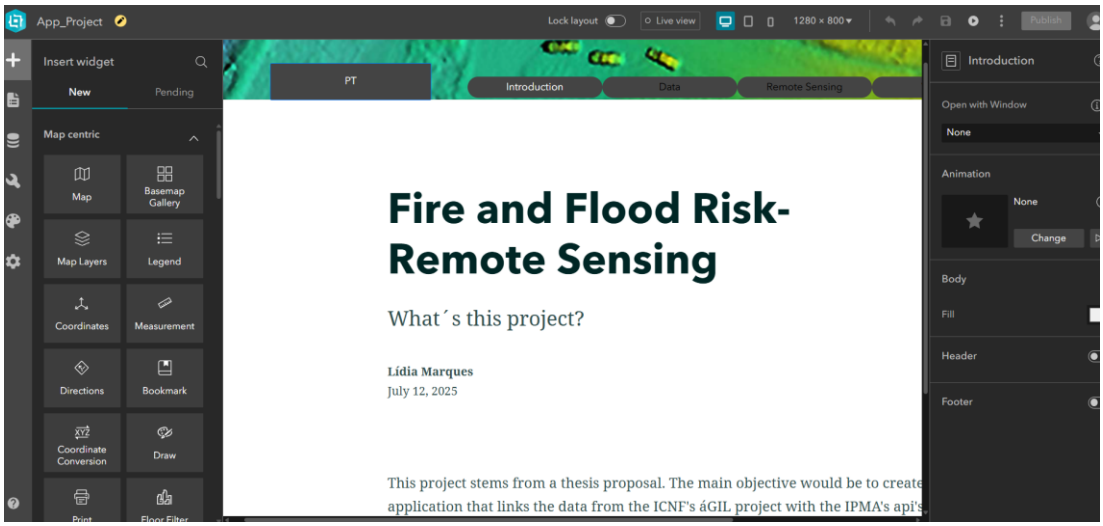

Figure 5-Experience Builder Interface

On the other hand, there is a free and open-source GIS application that allow users to create spatial datasets, manage them, analyse them and display them on a map, called QGIS (Figure 6). QGIS is a free, open-source platform with support for various data formats and easy integration with other open-source software. It offers high functionality for vector and raster operations through plugins and is designed as a standalone platform, while ArcGIS is commercial and not freely available [38].

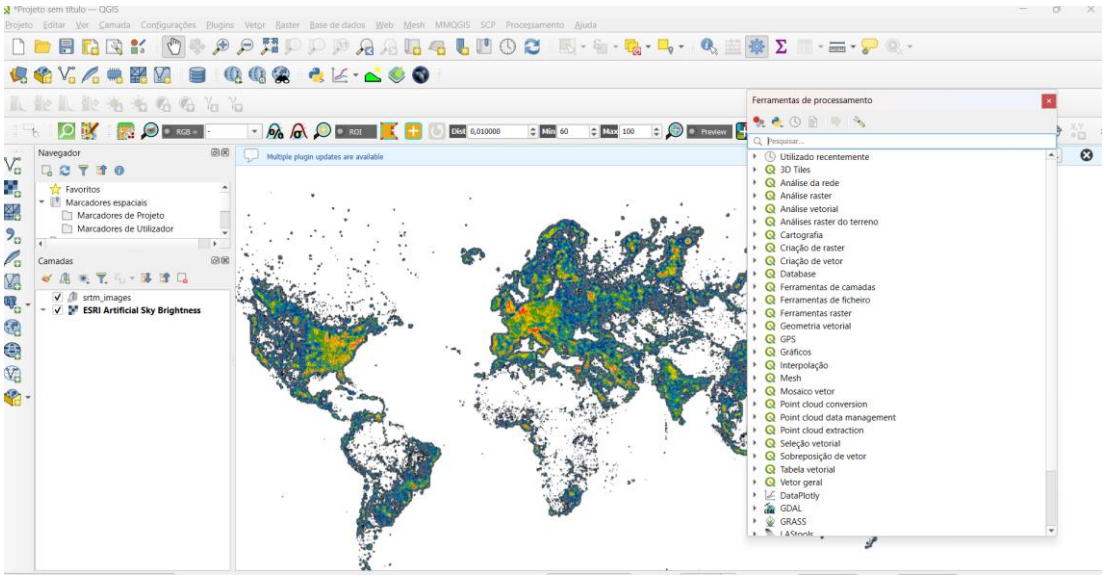

Figure 6-QGis Interface

3-Methodology

The thesis proposal was based on the creation of an interactive application that estimates and informs about fire and flood risk in each study area, corresponding to the seven regions of the Agile project. This application aimed to combine geospatial analysis with real-time meteorological data to support disaster risk assessment and decision-making. To achieve this, two main pillars were established: high-resolution LiDAR data provided by the Agile project, which enabled detailed characterization of the terrain and vegetation cover, and meteorological data obtained through the official IPMA APIs, which supplied up-to-date environmental conditions such as temperature, precipitation, wind speed, and humidity.

The development process relied on a combination of geospatial processing and programming tools.

ArcGIS Pro was used for LiDAR data processing, terrain modelling, and spatial analysis because of its advanced geoprocessing tools and efficient handling of large spatial datasets. In addition, ArcGIS Online served as the platform for hosting and sharing geospatial layers, providing easy access and collaboration capabilities for stakeholders. Meanwhile, QGIS was employed to provide complementary GIS functionalities, such as flexible data conversion and customizable visualization options, which enhanced the workflow. Finally, Anaconda Navigator was used to manage the Python environment for creating custom scripts, enabling the integration of IPMA API data with the processed LiDAR datasets in a reproducible and organized manner.

The ArcGIS Experience Builder was used as the environment for the application.

3.1. Data Sources and Understanding

3.1.1. LiDAR Data from Project Agile

The Agile Project was a Portuguese pilot initiative launched in April 2020 and completed in June 2021, funded by the Permanent Forest Fund of the ICNF (Instituto da Conservação da Natureza e das Florestas) and carried out in collaboration with ForestWISE and AGIF (Agência para a Gestão Integrada de Fogos Rurais). The project leveraged high-resolution

LiDAR imagery (5–10 points/m²) to generate specialized cartography detailing fuel loads (biomass), forest structure, quantity of woody material, stored carbon, and the distribution of infrastructure and buildings. Its main goal was to provide a robust basis for the creation of Decision Support Systems (DSS) in integrated forest and fire management, improving both strategic planning and operational response capacity.

The pilot implementation covered seven territories, encompassing approximately 45,000 hectares. These included diverse regions such as Monsanto Park, Mafra, Pombal, Sintra, Cascais, Proença-a-Nova, Oleiros, Serra da Lousã, and Vila Pouca de Aguiar. The dataset produced was organized into seven geographic segments corresponding to these territories, enabling targeted and location-specific analysis.

Among its key outputs, the Agile Project produced cartographic maps to assess forest density and structure, facilitated integrated evaluations of biomass, ecosystem services, stored carbon, and infrastructure, and contributed to identifying fire vulnerability levels and defence capacities. Furthermore, it supported the selection of priority areas for intervention, serving as a foundational element for public policies aimed at biomass valorisation and sustainable forest resource management.

The applicability of the LiDAR technology in the Agile Project was mostly evident in how it enabled quick and very precise territorial mapping, even under dense forest cover. The technology enhanced property identification processes' speed, with over 50% of the total area among the ten pilot municipalities covered in just 12 months. LiDAR also made land topography mapping possible, which made it possible to develop proposal algorithms for land configuration proposals, reconcile conflicts over simultaneous property claims, and test hypotheses regarding historical forest diversity and regimes of agriculture. Moreover, its precision and penetration capacity made it possible to have a potential for identifying old boundaries and concealed historical features, further clarifying the processes of landscape transformation over time [39].

3.1.2. Meteorological Data from IPMA APIs

IPMA provides a set of public Application Programming Interfaces (APIs) that supply meteorological, maritime, and seismic data. The APIs enable developers, researchers, and application systems to integrate refreshed environmental data directly into applications or workflows.

The data from IPMA APIs is exposed in JSON format through URL accessible endpoints to deliver interoperability and ease of integration in data processing workflows.

Forecasting data are obtained by automatic statistical post-processing of forecasts from two numerical models (ECMWF and AROME) and are updated twice a day, namely the 00UTC run (typically available from 10:00) and the 12UTC run (typically available from 20:00).

Datasets available include a broad range of environmental parameters, including:

• Meteorological Data – Hourly or daily forecasts by district or municipality, current atmospheric conditions (temperature, humidity, wind speed and direction, precipitation levels), UV index, and fire danger indices.

• Maritime Data – Sea state parameters such as wave height, water temperature, wind direction, and forecast for the coastal regions.

• Seismic Data – Earthquake detection in real time and archives of historical events for Portugal and the surrounding regions.

For this thesis, the selected API was "Observação Meteorológica de Estações (dados horários, últimas 24 horas)", which provides hourly meteorological observations from IPMA monitoring stations for the most recent 24 hours. This information includes parameters such as air temperature, relative humidity, wind speed and direction, and accumulated precipitation. This data is updated in near real-time, allowing it to be utilized in dynamic models for short-term environmental risk forecasting [40].

The integration of this API into the App allows LiDAR-derived environmental parameters (e.g., land slope or vegetation density) to be combined with real-time weather data, which allows for more accurate and timely prediction of fire and flood risk indices [41].

3.2-Data Preparation and Processing

For the preparation of the data and its processing, four steps were made.

1ST STEP:

Since ArcGIS Pro cannot process LiDAR data in the .laz format, which is a compressed version of the standard .las files, QGIS was used to convert the data from .laz to .las format. This conversion allowed the datasets to be fully compatible with ArcGIS Pro for further processing and spatial analysis (Figure 7).

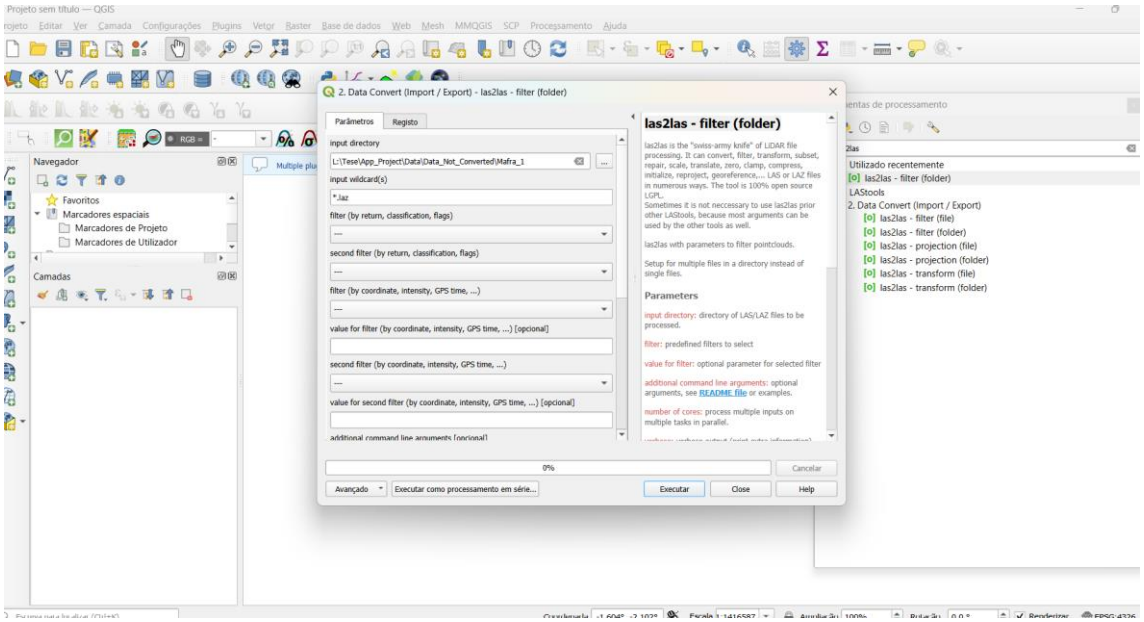

Figure 7-QGis Dashboard/ Environment

After that, the data were uploaded into ArcGIS Pro Software and the remaining steps were performed using the LAS Dataset to Raster tool, LAS to Multipoint tool and Point Density tools [42], [43], [44].

2ND STEP

We used the Las Dataset To Raster tool to calculate both the Digital Terrain Model (DTM) and the Digital Surface Model (DSM). Since the tool includes a parameter labelled "sampling type", it was necessary to determine an appropriate cell size [45], [46]. This cell size was calculated through Vegetation density and Average Point Spacing as you can see below:

To calculate Average Point Spacing (APS), we first need to determine Vegetation Density (*Dveg*). Vegetation Density is calculated as the ratio between the number of LiDAR points (*Nveg*) and the area that vegetation occupies (*Aveg*), as expressed in Equation 1. Once we determined the vegetation density, we can calculate Average Point Spacing (Equation 2).

Equation 1- Vegetation Density

$$Dveg = \frac{Nveg}{Aveg}$$

Equation 2- Average Point Spacing

$$APS \approx \frac{1}{\sqrt{Dveg}}$$

The figures illustrate key properties of the LiDAR datasets used in this study. Figure 8 shows the dataset's data source properties, including the total number of .las points. This information was used to estimate the point density, which is a indicator for vegetation density in each region. Figure 9 presents the dataset's spatial boundaries, including the coordinates of the bottom, left, right, and top extents. These coordinates were used to calculate the total area of each region. By combining the number of LiDAR points (which is the same as .las points) with the area, we were able to compute the LiDAR point density, which provides insights into vegetation structure and spatial distribution [47], [48], [49].

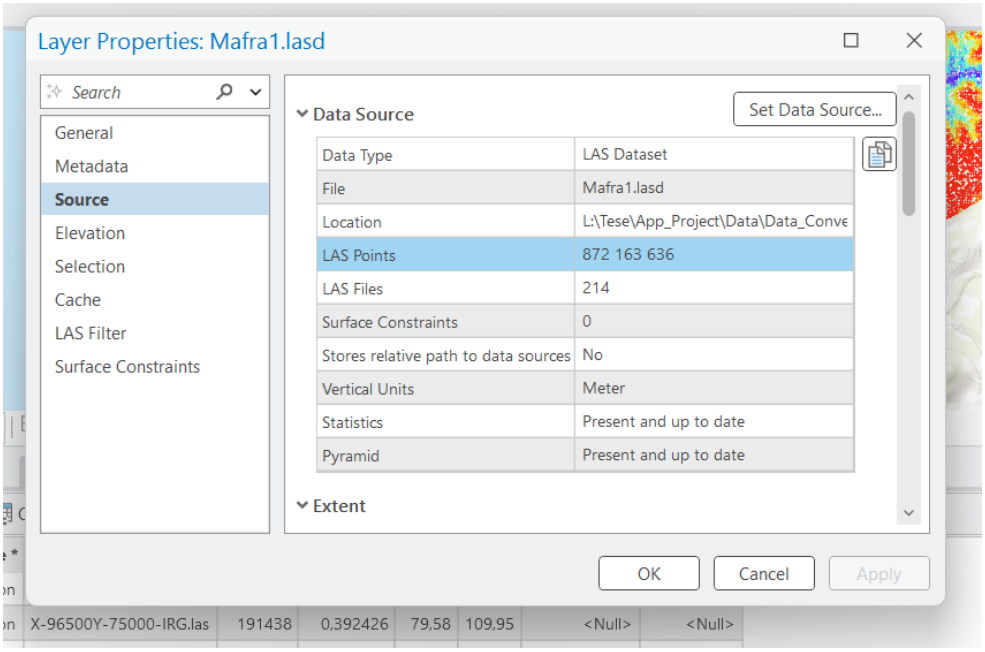

Figure 8-Data source properties of the LiDAR dataset, showing the total number of .las points, which were used to estimate vegetation density

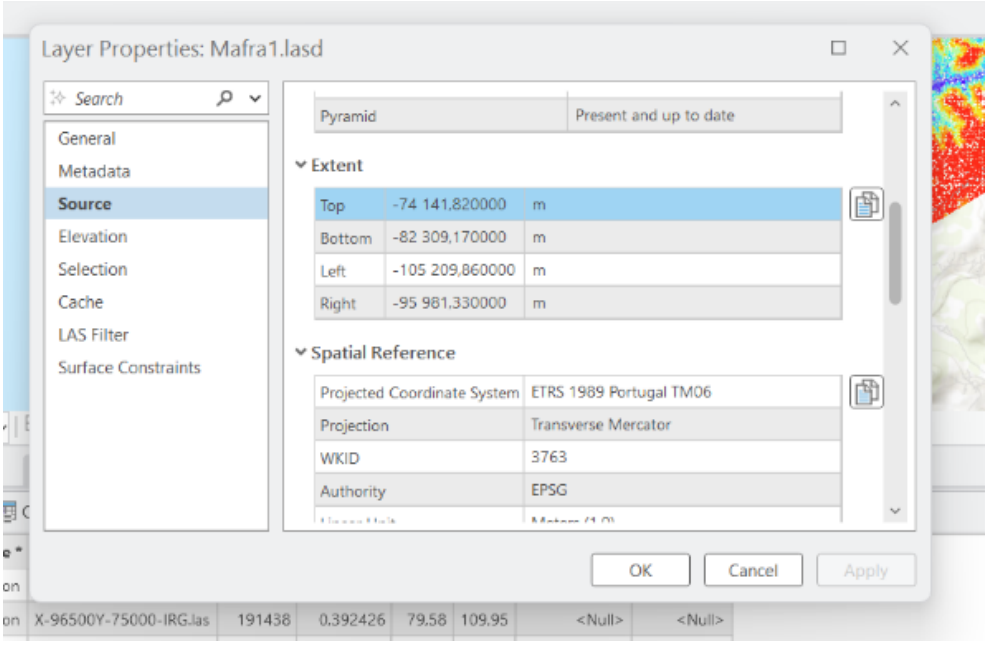

Figure 9-Spatial extent of the LiDAR dataset, indicating the bottom, left, right, and top coordinates, which were used to calculate the total area of the study region.

After we calculated Vegetation Density and APS, we were able to determine the cell size:

Equation 3- Cell Size

$$Cell\ Size \approx 2 \times APS$$

According to [50], the cell size should be equal to or greater than the Average Point Spacing (APS); therefore, the cell size was set to twice the APS.

Another parameter in the LAS Dataset To Raster tool is the Z Factor, which is used to convert vertical units to match the horizontal units of the dataset. Since both the LiDAR dataset and the map are in meters, a Z Factor of 1 was applied, ensuring consistency between horizontal and vertical measurements.[51].

3rd and 4th Step:

To calculate Point Density (Vegetation Density), first we had to use Las to Multipoint (ArcGIS Pro Tool), and the main label of this tool was Average Point Spacing.

After that to use Point Density tool. We had to choose Las To Multipoint Output as Input of this tool.

To preprocess the LiDAR data, the LAS to Multipoint tool was applied (Figure 10). This tool converts LAS datasets into multipoint features, allowing their subsequent visualization and analysis in ArcGIS Pro. Afterwards, the Point Density tool was used (Figure 11) to calculate the density of point features within a neighbourhood around each output raster cell. This step provides a spatial representation of point concentration, which is essential for identifying areas with higher data/vegetation density [44].

As you can see in figure 11, we had to calculate radius, so we calculate as follows:

To find a radius it is necessary to choose a radius proportional to the average density of the points [52].

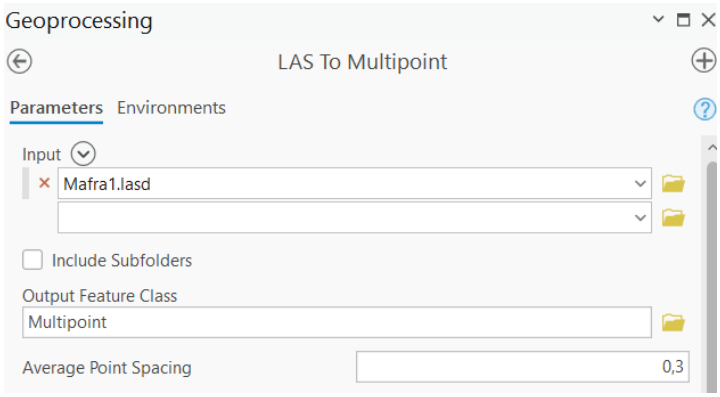

Figure 10-Las To Multipoint tool

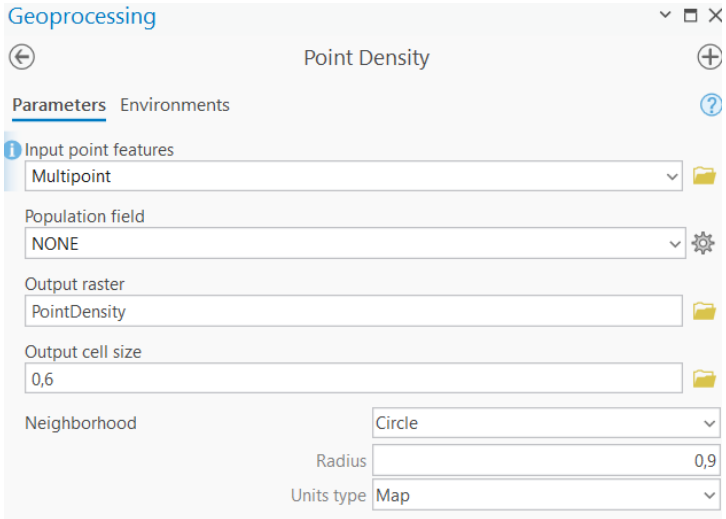

Figure 11-Point Density Tool

When the article states that the search radius should be proportional to the average density of the points, this indication should not be understood literally, that is, as a direct multiplication of the density (points per unit area) by a factor. Density is an area measure,

while radius is a linear measure. Therefore, the correct interpretation of this recommendation is that the average density serves only as an indirect indicator of the average spacing between points. Thus, what is effectively at issue is the use of APS, which translates density into terms of average distance between points [52].

To estimate the search radius used in the Point Density calculation, the following approximation was adopted:

Equation 4-Radius Estimation

$$Radius \approx K \times APS$$

The official documentation of ArcGIS Pro indicates – "Larger values of the radius parameter produce a more generalized density raster. Smaller values produce a raster that shows more detail", where APS is the average distance between LiDAR points in the dataset, and K is a scaling coefficient. This approach is in line with the general guidance in the ArcGIS Pro documentation for the Point Density tool, which indicates that larger radius values produce a more generalized density raster, and smaller values yield more detail [44].

So, to maintain more detail and make the radius larger than the cell size (if we multiply by 2, the values of the radius will be equal to the cell size), it was decided to assign K a value of 3.

Equation 5-Radius

$$Radius \approx 3 \times APS$$

Table 1 summarizes the results of the calculations of cell size, radius, and average point spacing between points for all regions of the Agile Project. The methodology applied to each region was identical to the procedure described above for the Mafra region. The table allows a direct comparison of the parameters calculated in the different study areas.

Table 1-Summary of Cell size, APS, and radius for the seven study regions

	Mafra	Monsanto	Pombal	Proença-Oleiros	Serra da Lousã	Sintra-Cascais	Vila Pouca de Aguiar
Cell Size	0,6	0,62	0,56	0,68	0,82	0,6	0,9
APS	0,3	0,31	0,28	0,34	0,41	0,3	0,45
Radium	0,9	0,93	0,84	0,102	1,23	0,9	1,35

3.3. Definition of Risk Evaluation Parameters

The definition of the parameters used to evaluate fire and flood risk was guided by methodologies reported in the scientific literature. The specific parameters and their sources are described individually, which are detailed in the following sections:

Fire Risk Parameters

Wildfire risk is influenced by a combination of climatic variables and vegetation characteristics. For this project, the main parameters considered were:

- Slope- The slope criterion directly impacts forest fire risk and danger. Forest fire risk refers to the possibility of a forest fire due to human activities or natural causes, while forest fire danger is the danger posed by a thick, lively flammable community, increasing fire severity and extinguishing difficulties. Meteorological and topographic parameters also directly affect fire danger. Slope is one of the most important factors affecting forest fire danger as it increases the speed of fire spread, flammable material type, and severity. Studies show that as slope increases beyond the low slope range of 0–10%, both forest fire risk and danger tend to increase [53].

- Aspect- Aspect significantly influences vegetation and fuel complex in mountainous terrain, affecting the amount of solar radiation incident upon mountain slopes. This, in turn, influences the composition of vegetation, with plant communities on south-facing slopes being more xerophytic and less dense. Seasonal and diurnal variations, such as snow melt and herbaceous fuel cure-out, also contribute to fire hazard. Aspect's influence is evident in fire occurrence, with studies showing greater number of ignitions and large fires on southerly aspects [54].

- Height and Density -Wildfire potential depends on the height and density of the fuel. Areas with tall and densely packed vegetation promote rapid fire spread and higher fire intensity, as the abundance of continuous fuel allows flames to propagate more easily through the canopy and understory. In contrast, stands with

lower density or shorter vegetation exhibit slower fire spread and lower intensities due to discontinuities in the fuel structure. This relationship between vegetation structure and fire behaviour has been documented in article [54].

- Temperature- The temperature of forest significantly influences wildland fires. It directly affects the flammability of fuels and indirectly influences fire behaviour through factors like wind, fuel moisture, and atmospheric stability. Understanding local temperature variations is crucial for understanding fire behaviour [55].
- Humidity - Humidity plays a crucial role in fire weather, directly affecting the flammability of forest fuels and indirectly affecting other aspects of fire behaviour. It is exchanged between the atmosphere and dead wildland fuels, with dry fuels absorbing moisture and giving it to dry air. Humidity also influences surface temperatures, including surface fuel temperatures, by controlling radiation and reflecting and radiating heat energy. Moisture is necessary for the development of lightning, which is a dreaded cause of wildfires in mountainous areas. Atmospheric humidity, measured using a psychrometer, represents the actual moisture in the air and relative humidity indicates the degree of saturation at a given temperature [55].
- Wind Intensity- The rate of spread of a wildfire increases markedly when a wind springs up [56].The interaction between fire and wind is crucial in fire science, as fire strongly distorts downstream airflow. Extensive surveys have been conducted to explore the various behaviours of wildfires in both still air and windy conditions. And the conclusion is the wind can significantly affect the design of fire safety procedures for structures, and this has not been addressed in previous reviews [57].

  Wind has a significant impact on fire behaviour due to the fanning effect, which increases the source of oxygen, reduces the humidity of the surface fuel, and causes firebrands, sparks, and flames to move and reach new sources of fuel. Wind damage increases the amount of flammable fuels, intensifying the fire and resulting in unanticipated changes in vegetation composition. Topographic slope and wind direction are significant factors that determine the direction and spread rate of wildfires [57].

Flood Risk Parameters

Flood hazard assessment typically integrates hydrological and topographic indicators. In this project, the following variables were considered to calculate the risk of flood:

- Flow direction- flow direction determines the accumulated drainage area (flow accumulation), which comprises a raster layer with each pixel's attribute representing an upstream contribution area. Slope is an important indicator of flood-prone surface zones, as it affects the speed at which water flows through drainage channels and watersheds. The drainage network is established based on the cumulative drainage area, calculated by applying a threshold to the accumulated area. Soil characteristics are essential for delineating groundwater potential in study areas, as they control rates of infiltration, percolation, and permeability. To calculate flow direction, the calculation of the fill is needed [58].

- Topographic Wetness Index (TWI)- Flood hazard maps and depth in rivers are complex processes in hydrology, with both geomorphological and hydraulic procedures being imperfect at watershed scale. Researchers have demonstrated that a topographic wetness index (TWI) via a maximum likelihood estimation procedure applied to the results of a hydraulic inundation model can be useful for hazard zoning of potentially flood-prone areas in micro and meso scale. In this context, micro-scale refers to small areas such as local catchments or specific landscape features (meters to hundreds of meters), while meso-scale corresponds to sub-watersheds or small watersheds (hundreds to thousands of meters). The TWI thus provides a tool to identify and quantify areas prone to flooding across these scales [59].

- Surface Curvature-Surface curvature plays a significant role in determining the risk of floods since land morphology influences biodiversity, agricultural production, and economic activity, and its use and management directly influence flood genesis [60].

- Vegetation height- Flood drainage ditches and vegetation play a crucial role in preventing floods by controlling water flow and directing it away from property

and communities. Vegetation acts as a natural buffer against floods, holding soil in place and reducing erosion. It also increases water absorption, reducing the risk of flooding. Planting vegetation near a flood drainage ditch not only provides a barrier to water flow but also filters water, removing pollutants [61].

- Accumulated precipitation - The study explores the relationship between extreme precipitation and flood intensities in response to global warming, focusing on the Northern Hemisphere mid-latitudes with a strong seasonal cycle of water availability. Extreme precipitation changes have a clear connection with seasonal water availability. The study also examines the response of precipitation and flood extremity to spatial and seasonal variations of water availability.

  The results show that extreme precipitation and flood changes in different climate regions converge for more extreme events due to a faster increment of the increases with event extremity in drier climates. The percentage area of wet land areas with an increasing intensity signal of extreme precipitation remains almost constant when events become more extreme, while the percentage area of drier regions with an increasing flood intensity signal rises larger with event extremity [62].

- Atmospheric pressure and wind- Article [63] explores the role of atmospheric pressure and wind in influencing storm surges and coastal flooding probability along the Atlantic coast of France. The research uses long-term tide gauge records and meteorological datasets to assess the mechanisms and trends influencing coastal flood hazard. The study found that low atmospheric pressure and strong onshore winds are principal determinants of positive surge events in the region.

3.4. Data Integration and Model Development

To illustrate the process of integrating multiple data sources into the risk assessment model, Figure 12 presents the conceptual workflow. Static variables derived from LiDAR data, such as terrain and vegetation characteristics, are combined with dynamic variables from IPMA APIs, including meteorological conditions. These inputs are integrated through a weighted risk index model, with the outputs visualized in the final application. The integration process aimed to combine terrain characteristics derived from LiDAR with weather data obtained from the IPMA API, to calculate fire and flood risk indices for the seven regions covered by the Agile Project.

Figure 12 illustrates the general workflow of this integration, from data preparation to publication and visualization in the final application.

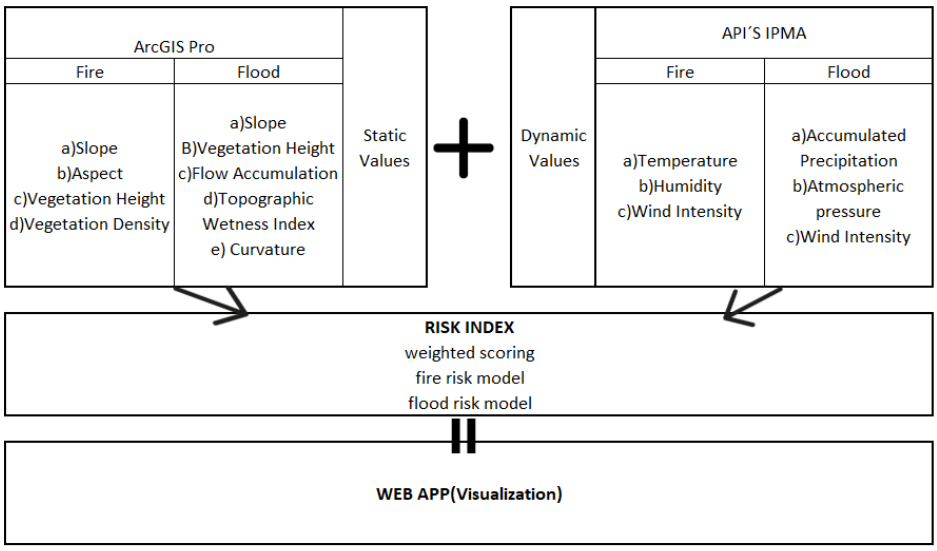

Figure 12-Conceptual workflow of data integration. Static variables derived from LiDAR (terrain and vegetation) and dynamic variables from IPMA APIs (meteorological conditions) are combined through a weighted risk index model, with outputs visualized

Using ArcGIS Pro tools, various terrain variables such as slope, aspect, and flow accumulation were calculated. However, only three datasets were derived from the original data: DTM, DSM, and the LAS to Multipoint. From these base products, a set of essential topographic and vegetation-related variables was derived, including slope, aspect, curvature, vegetation height, topographic wetness index (TWI), and point density. Figure 13.

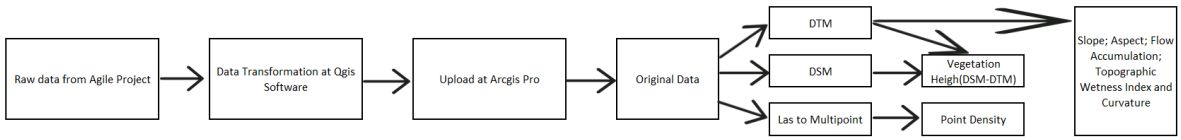

Figure 13-Data Workflow

After that the municipalities of interest were clipped and extracted from CAOP (Carta Administrativa Oficial de Portugal) shapefile, a file containing the districts, municipalities and civil parishes (Freguesias), we made that for the seven regions and in the end, we make a shapefile including all the 21 municipalities that the data reached. This ensured that all indicators were spatially constrained to the study areas.

Step 1: ArcGIS Pro allows us to use all kind of spatial reference system, but to avoid different spatial reference system at ArcGIS online, we had to change from ETRS_1989_Portugal_TM06 to WGS 1984 Web Mercator (Auxiliary Sphere), which is the default system for online visualization in ArcGIS Online. This harmonization guaranteed that the resulting datasets could be published and displayed without inconsistencies [64].

Step 2: Meteorological information was obtained through the IPMA API´S, which provides data in JSON format with hourly updates. The available variables included air temperature (°C, hourly mean at 1.5 m, e.g., 20 °C), relative humidity (% at 1.5 m, e.g., 60 %), wind speed (km/h at 10 m, e.g., 15 km/h or m/s, e.g., 4.2 m/s), wind direction (classified into 8 main directions: N, NE, E, SE, S, SW, W, NW), accumulated precipitation (mm, hourly, e.g., 2 mm), atmospheric pressure (hPa, reduced to mean sea level, e.g., 1013 hPa), and solar radiation (kJ/m², hourly, e.g., 500 kJ/m²).

Each station was spatially referenced and then associated with the corresponding municipality. This step ensured that the most representative meteorological data was linked to each study area.

Step 3: The core of the integration process was the development of a risk index model, carried out using a Python script.
Since no single study encompassed all the variables used, the model was designed based on a synthesis of findings from multiple scientific articles.
For fire risk, the model considered variables such as slope, aspect, vegetation height and density, temperature, humidity, wind intensity, and solar radiation. For flood risk, the selected parameters included topographic slope, vegetation height, flow accumulation, topographic wetness index, and curvature. The variables from the IPMA API included accumulated precipitation, atmospheric pressure, and wind intensity.

The approach followed a weighted scoring methodology, in which each variable contributed to the final risk score according to weights and thresholds based on scientific literature. This allowed the generation of synthetic indices capable of reflecting the relative susceptibility of each area to fire or flooding.

Step 4: The Python script can refresh the values of specific fields in the shapefile each time it is executed, updating the previously shared data in ArcGIS Online. The refreshed fields include rcm (calculated risk index), update_date (date of the latest update), and risk (risk classification).

Step 5: These were then consumed by an interactive application developed in ArcGIS Experience Builder. Resulting in our final application.

4. Application Development

4.1. System Architecture

To provide an overview of the implemented solution, including data preprocessing, integration, and visualization, the system architecture is illustrated in Figure 14. This figure shows how LiDAR data is processed in ArcGIS Pro, shared in ArcGIS Online as feature layers, and then combined with meteorological data using Python, which is subsequently consumed in the interactive dashboard in Experience Builder.

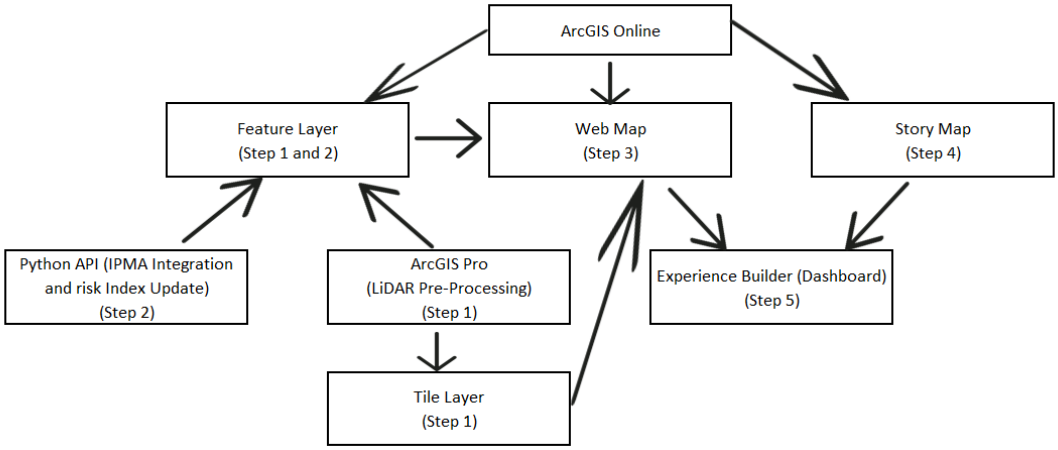

Figure 14-System architecture of the implemented solution. LiDAR preprocessing in ArcGIS Pro and meteorological data integration through Python feed ArcGIS Online, which hosts feature layers later consumed in the Experience Builder interactive dashboard.

The system architecture, figure 14 had the following steps:

Step1: ArcGIS Pro was the main environment used for processing LiDAR data. In this stage, raw point cloud datasets were converted and processed to generate derived rasters and indicators, such as slope, aspect, vegetation height, vegetation density, flow accumulation, curvature, and topographic wetness index (TWI).

Once calculated, the aggregated indicators for each municipality were exported as feature layers and shared with ArcGIS Online, where they became available as hosted services.

ArcGIS pro also created a tile hosted layer that only aggregated the seven regions and the static variables. After that we also save it as a web map, to incorporate that in the final dashboard.

Step 2: To incorporate meteorological information, a Python script was developed within the Anaconda environment. This script accessed the IPMA Observation Stations API, collected the latest meteorological data, and applied the risk index calculation algorithm.

The script continuously merged static terrain features with dynamic meteorological variables, updating the respective feature layers stored in ArcGIS Online. This ensured that the data feeding the application remained timely and consistent whenever is executed.

Step 3: The feature layer was transformed into a web map for two main reasons. First, the Experience Builder dashboard does not support feature layers directly, as there are no widgets designed to work with them. Second, we needed to style the final map according to specific visualization requirements, which is only possible using the ArcGIS Web Map tool. Hosted feature layers alone do not allow this level of customization.

Step 4: We created through ArcGIS Online the Story Map. This app let us explain what the application is all about and, what we can find in all the application tabs.

Step 5: The final component of the system was the web application built in ArcGIS Experience Builder. This environment allowed the integration of web maps, and story maps into an interactive interface accessible to end users.

Through Experience Builder, users can dynamically visualize fire and flood risk indices, explore thematic maps, and monitor real time conditions updated via the IPMA API. The dashboard-based design provided an intuitive decision-support tool, consolidating the entire workflow into a single platform

4.2. LiDAR Data Processing Workflow

4.2.1. Using ArcGIS Tools

As the data is all separated on the ICNF website it was decided to create seven projects in ArcGIS Pro [39]. And from each project containing each dataset, three main outputs were calculated from the "raw" data: DTM, DSM, and point density. Then, the following ArcGIS Pro tools were used based on the DTM: Slope, Aspect, vegetation height, flow accumulation, topographic wetness index, and curvature.

As the Slope, Aspect, and Curvature parameters are part of the ArcGIS tools, we are not going to dive into them [65], [66], [67].
But the remaining we had to calculate them in different ways, as it is explained bellow:

4.2.1.1. Vegetation Height:

To calculate vegetation height, we used raster calculator tool at ArGIS Pro as you can see in figure 15:

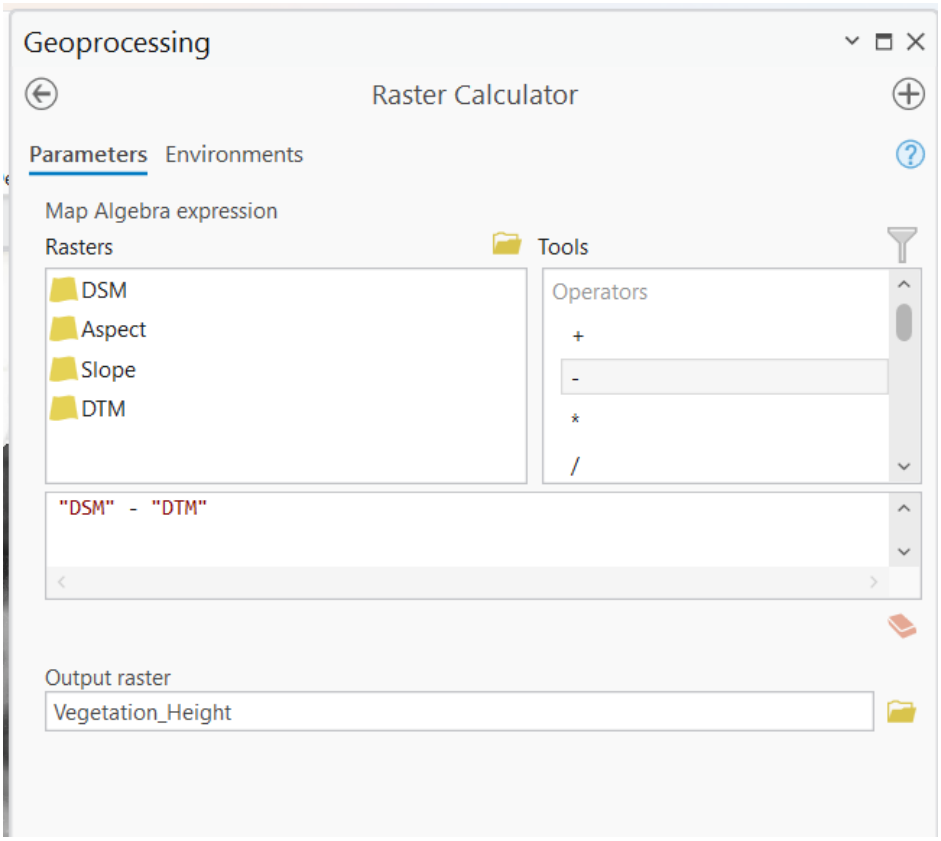

Figure 15-Raster Calculator tool

The Raster Calculator tool in ArcGIS Pro is a geoprocessing tool used to perform map algebra on raster datasets. It allows users to combine multiple raster layers using mathematical, logical, and conditional operations to generate new raster outputs. This tool is particularly useful for environmental modelling and hazard mapping, as it enables the calculation of indices, reclassification of data, and integration of multiple spatial variables into a single risk or suitability layer [68].

As explained at DTM (in meters) and DSM (in meters) literature from ArcGIS documentation, DSM calculates the major point of the data, and DTM, the minor point of it. So, the calculation of the vegetation height (in meters) comes as follows:

Equation 6-Vegetation Heigh

$$Vegetation\ Height = DSM - DTM$$

4.2.1.2. Flow Accumulation

As mentioned earlier, to calculate flow direction and flow accumulation, it is necessary to use a hydrologically correct DTM that ensures continuous surface runoff without interruptions caused by artificial depressions. These depressions, also called sinks, can result from interpolation errors, data noise, or resolution limitations. A hydrologically correct surface is obtained by removing or filling these sinks, allowing for accurate calculation of flow directions and accumulation.

The Fill tool in ArGIS Pro corrects this problem by filling in unwanted depressions. According to Esri's official documentation, the z-limit parameter controls the maximum depth of depression to be filled:

- z-limit = 0 (or empty): all depressions are filled.
- z-limit > 0: only depressions shallower than the specified value are corrected.

For hydrological analyses, the recommended practice is to use z-limit = 0, ensuring that no artificial depressions interrupt the flow (Esri, Fill (Spatial Analyst)). So, we calculated Fill that way.

Figure 16 illustrates the workflow for hydrological analysis using DTM. In panel (a), the Fill [69] tool is applied to remove artificial depressions (sinks) in the DTM, ensuring a hydrologically correct surface where surface runoff can flow continuously. Panel (b) shows the Flow Direction raster [70], which indicates the direction of surface water movement across the terrain, derived from the filled DTM. Panel (c) presents the Flow Accumulation raster [71] , highlighting areas where surface runoff accumulates, with higher values representing locations that receive water from larger upstream areas. This sequence demonstrates how the DTM is processed and analysed to model surface water flow accurately.

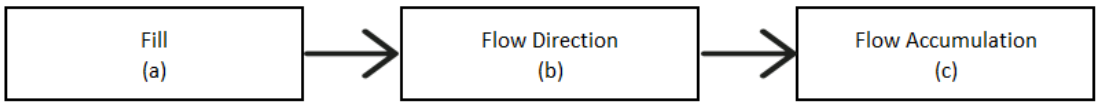

Figure 16-Hydrological analysis using DTM. (a) Fill tool applied to remove depressions in the DTM, ensuring a hydrologically correct surface. (b) Flow Direction showing the direction of surface water runoff. (c) Flow Accumulation indicating the accumulated amount

4.2.1.3. Topographic Wetness Index (TWI)

According to article [72] TWI is calculated as follows:

Equation 7-Topographic Wetness Index

$$TWI = \ln\left(\frac{a}{\tan\beta}\right)$$

where:

• "a" is the specific catchment area – "a indicates how much land 'drains' into that cell, measured in square meters per meter." "High values of a mean that a lot of water converges at the point → greater potential saturation; low values → little contribution → less saturation."

• "β" is the local slope in radians.

The calculation of a is described in article [73].

How to calculate a in a raster (regular grid)

• First, calculate the Flow Accumulation (FA) in ArcGIS Pro. This raster indicates how many upstream cells contribute to each cell.

• To obtain the total upstream area (A) in m²:

Equation 8-Total upstream area

$$A = (FA + 1) \times Cell\ Size^2$$

Here, +1 includes the cell itself, and cell size squared is the area of each cell.

Next, divide A by the length of the cell perpendicular to the flow (≈ cell size) to obtain the specific contribution area:

Equation 9-Specific contribution area

$$a = \frac{A}{cell\ Size} = (FA + 1) \times cell\ Size$$

The cell size value exists at the Flow Accumulation properties.

Slope radian is calculated as follows [74]:

Equation 10- Slope (Rad)

$$Slope\ (Rad) = \frac{\pi}{180°} \times Slope$$

TWI is calculated as shown in equation 7, when using raster data, a can be derived from the flow accumulation raster (FA). The calculation of a is made through the formula demonstrated in equation 8 and dividing by the cell size to obtain per-unit contour length gives the equation 9. Therefore, the TWI calculation integrates both the topography-controlled accumulation area and the local slope, allowing the quantification of potential water accumulation in each raster cell.

Giving an example:

- If $a = 500$ meters $\beta = 0.2$ rad ($\approx 11.46°$).

Equation 11-Example of a TWI calculation

$$\text{TWI} = \ln\left(\frac{500}{\tan 0.2}\right) \approx \ln(2500) \approx 7.82$$

The calculated TWI value of 7.82 is dimensionless, as it is derived from the natural logarithm of the ratio between the upward contributing area and the tangent of the local slope. Higher TWI values indicate locations with greater potential for water accumulation, while lower values correspond to drier areas. Thus, the TWI provides a relative moisture index rather than a physical measurement with specific units.

4.2.2. Creating the final shapefile

To enable the integration of all processed data into the interactive dashboard, it was necessary to create a final shapefile that consolidate the risk information for each study area. These shapefiles allow the results to be easily shared and visualized in ArcGIS Online. To create them, we used the CAOP shapefile as a base, in this case we only used the municipalities of it. The risk values calculated from LiDAR and meteorological data were joined to this base to generate the final geospatial datasets ready for visualization and further analysis.

4.2.2.1. CAOP shapefile:

CAOP 2023 is Portugal's Official Administrative Map launched that year, a cartographic document from the Directorate-General for Territory (DGT) that records the boundaries and delimitation of the country's administrative districts, including districts, municipalities, and civil parishes [75].

This dataset is publicly available as vector files, which we used as a base for spatial analysis and data integration. In the context of this work, the CAOP shapefiles allowed us to associate meteorological and LiDAR-derived variables with specific administrative units, generating final shapefiles containing fire and flood risk information per municipality, which were subsequently visualized in ArcGIS Online.

4.2.2.2. Clipping and extracting municipalities from CAOP shapefile:

From the file we only used “Cont_Mun_CAOP2023.shp”, and from that shapefile we clipped and extracted our municipalities of interest within each of the seven Agile project regions, The municipalities were chosen based on the maximum area covered by the data. In other words, there were municipalities that were covered by the data and were also included in this study (Table 2).

Table 2-Study area divided by municipalities

Region/Study Area	Municipalities
Mafra	Mafra
Parque Florestal de Monsanto	Oeiras; Amadora; Lisboa
Pombal	Leiria; Ourém; Pombal
Proença-Oleiros	Proença-a-Nova; Oleiros; Sertã; Castelo Branco
Serras da Lousã	Lousã; Miranda do Corvo; Figueiró dos Vinhos; Castanheira de Pêra; Góis
Sintra-Cascais	Sintra; Cascais
Vila Pouca de Aguiar	Vila Pouca de Aguiar; Ribeira de Pena; Boticas

4.2.3. Reclassify the variables

After we clipped and extract the municipalities of our interest, we had to use another tool in ArcGIS Pro named Reclassify (Figure 17).

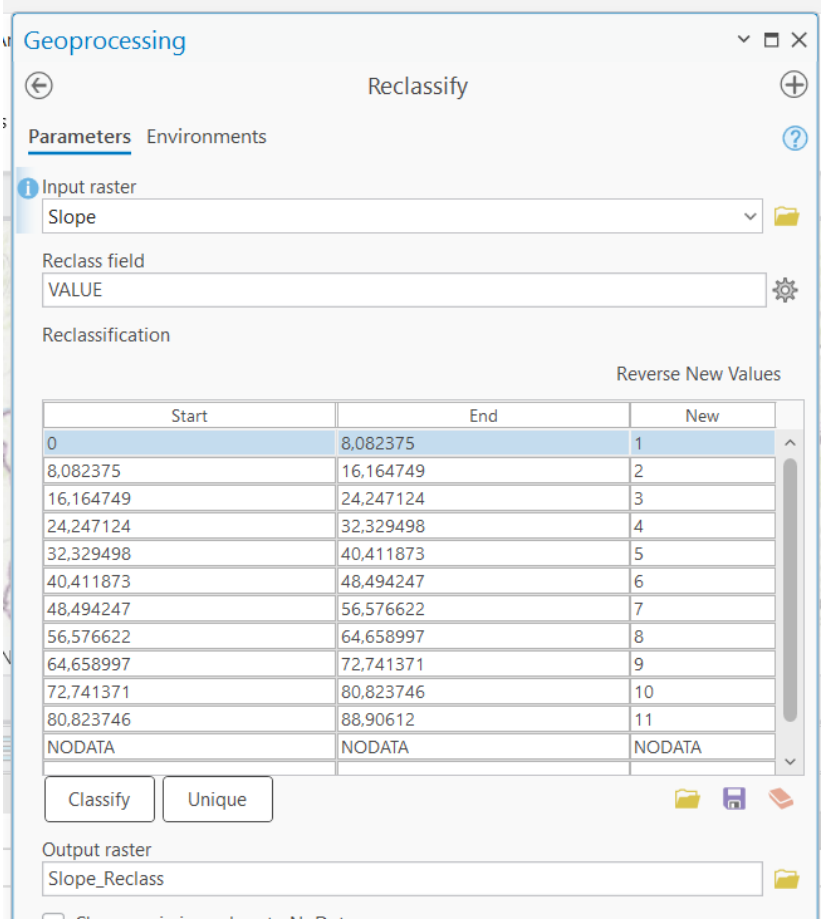

Figure 17-Reclassify

The Reclassify tool in ArcGIS Pro was used to transform continuous raster datasets, such as slope, vegetation height, and Topographic Wetness Index (TWI), into discrete classes for the fire and flood risk assessment [76].

"Reclassification is a method of changing the attribute values without altering the geometry of the map. In fact, it is a database simplification process that aims at reducing the number of categories of attribute data layer. Accordingly, features adjacent to one another that have a common value will be treated and appear as one class. Reclassification is an attribute generalization technique. After reclassification, the common boundaries between polygons with identical attribute values are dissolved and rebuilt the topology." Affirming that: "Buffer zone creation and reclassification are some of the important techniques in geographic analysis" [77].

In essence, reclassification allows us to assign a new value to each cell in an input raster based on a predefined classification.

This process is crucial for risk modelling. Instead of dealing with hundreds of slope values or other values, reclassification reduces the complexity to just five risk classes (Low, Moderate, High, Very High, Extreme). This allows the application of a specific weights or criteria to each class, facilitating the final calculation of suitability or risk. For example, an “Accentuated” area will have a higher weight in fire risk model due to the speed of fire spread, while a “Flat” area will have a lower weight.

Reclassification is therefore a bridge between the complexity of reality and the simplicity of a decision-making model.

4.2.4. Fusion of the variables into the Shapefile

4.2.4.1. Creation of the Table using Zonal Statistics as Table

To integrate the data from the tools, slope, aspect, vegetation height, etc with the CAOP shp, we had to use zonal statistics as table tool.

According to the ESRI documentation, zonal statistics tables are used to create connection points between the raster and the CAOP shapefile. Subsequently, using join fields, the values will go to the shapefile. This allows the slope, aspect, etc. values to be organized in the shapefile, which we will later share with ArcGIS Online [78], [79].

As shown in Figure 18, it was necessary to select a specific statistics type, and Table 3 presents all the corresponding results. The decisions made during this process were guided by the documentation referenced in [48], [80], [81], [82]. The selection of zonal statistics presented in Table 3 follows established best practices in spatial analysis and environmental modelling, as different variable types require specific statistical treatments.

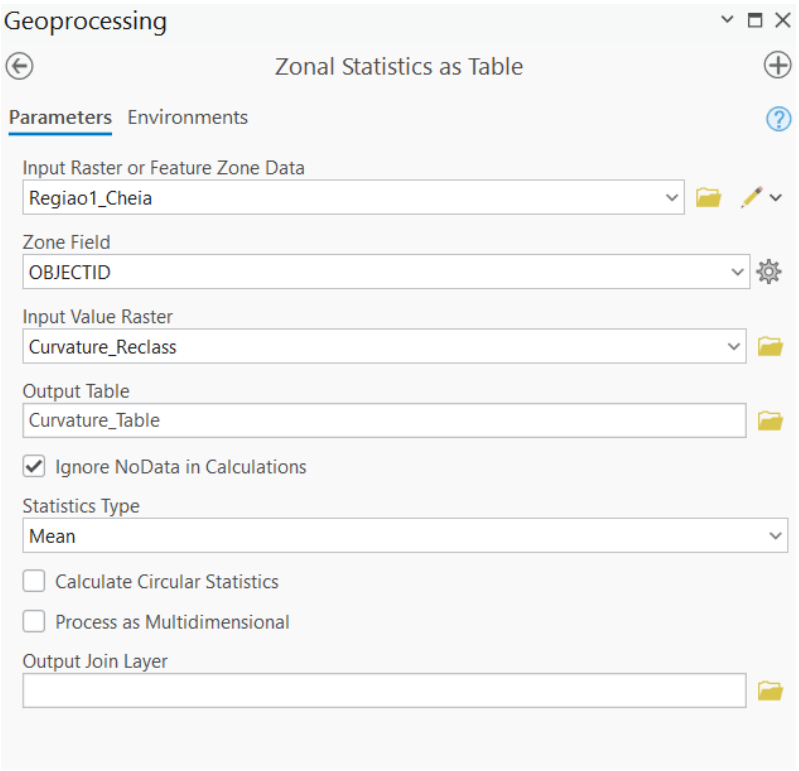

Figure 18-Zonal Statistics as Table

Table 3-Statistics Type

Data Type	Variables	Ideal Statistics	Reason
Continuous	Slope, Vegetation Height, Curvature and TWI	Mean	The average value provides a general and robust representation for the entire area. It provides a single value that smooths out extremes and allows for a fair comparison of the slope or height of vegetation between study areas of different sizes.
Categorical	Aspect	Majority	The "aspect" measures the direction (e.g., North, South, East). The average of directions has no physical meaning. The majority is the only option that identifies the most common direction in an area, which is a key factor for sun exposure and wind speed.
Accumulation	Flow Accumulation	Sum	The main objective of flood analysis is to determine the total amount of water converging at a given point. The sum aggregates all water flow values for a given area, providing a direct measure of the volume and risk of flooding.
Density	Point Density	Mean	The Point Density tool already creates a surface with continuous density values. The average value of this surface within a zone gives the average concentration of points per unit area, which is the most relevant indicator for the risk of events such as fire ignitions.

Figure 19 shows an example of a table resulting from the use of the Zonal Statistics as Table tool. This table corresponds to the Vila Pouca de Aguiar project, which is why it includes only three municipalities. For this table, the slope values were summarized using the mean, while for other variables, such as aspect, the majority statistic would be applied to capture the most frequent category within each zone.

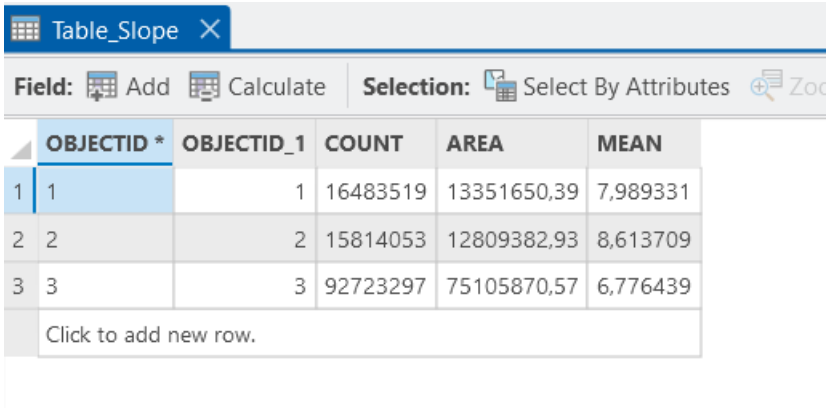

Figure 19-Table slope

4.2.4.2. Adding table values to shapefile using Join Field Tool

The Join Field tool is used to integrate the results obtained in the statistics table (generated by Zonal Statistics as Table) into the original shapefile. A common field, like ObjectID, is used for the join, guaranteeing that each polygon receives the computed statistical values (e.g., Mean Slope, Majority Aspect, etc.) accurately. This makes spatial analysis and integrated data visualization easier by allowing all variables that are derived from the rasters to be stored directly in the shapefile attribute table.

As previously mentioned, it was determined to split the projects into seven (Point 3.5) to facilitate the creation of the final shapefiles. However, to share with ArcGIS Online, only one shapefile will be shared. For this, we use the merge tool.

The Merge tool in ArcGIS Pro is a geoprocessing tool that combines multiple datasets of the same type (either feature classes or tables) into a single, new output dataset. According to Esri documentation, it is commonly used to integrate data from different sources while maintaining all the original attributes [83].

Then we shared 4 shapefiles (we shared Fire and Flood shapefile twice, once in Portuguese and the second in English respectively) (Table 4 and 5).

Table 4-Fire Shapefile

OBJECTID	DICO	Municipio	Distrito	MEAN_Slope	MAJORITY_	MEAN_Vegetation_Height	MEAN_Density
1	1109	Mafra	Lisboa	2,502335571	8	2,718715806	1,053698305
2	1106	Lisboa	Lisboa	3,872228246	6	3,441915776	1,022349693
3	1110	Oeiras	Lisboa	3,698968864	5	3,313192559	1,00535765
4	1115	Amadora	Lisboa	3,732117156	5	3,144993308	1,002588452
5	1015	Pombal	Leiria	5,600596048	8	2,074555262	1,119921674
6	1009	Leiria	Leiria	5,711636894	7	1,593047449	1,083609142
7	1421	Ourém	Santarém	5,810014129	7	2,114226692	1,038383214
8	0502	Castelo Branco	Castelo Branco	7,745810928	4	2,127583536	1,001963161
9	0506	Oleiros	Castelo Branco	7,067573032	8	2,616957066	1,000550177
10	0508	Proença-a-Nova	Castelo Branco	6,931201189	5	2,672467058	1,000552922
11	0509	Sertã	Castelo Branco	7,315960943	5	2,647674658	1,000909087
12	0606	Góis	Coimbra	7,7756143	3	3,61266691	1,008488273
13	0607	Lousã	Coimbra	7,106705894	9	3,607213767	1,014253761
14	0609	Miranda do Corvo	Coimbra	7,885436182	7	3,693822165	1,00643371
15	1007	Castanheira de Pêra	Leiria	7,068745481	6	3,323612873	1,010593133
16	1008	Figueiró dos Vinhos	Leiria	7,144869123	6	3,298921444	1,002613205
17	1105	Cascais	Lisboa	5,044513002	6	2,410436482	1,031186492
18	1111	Sintra	Lisboa	5,394534189	8	2,904765655	1,101143474
19	1702	Boticas	Vila Real	7,989331404	5	3,644708061	1,049127587
20	1709	Ribeira de Pena	Vila Real	8,613708959	7	3,650463511	1,035862882
21	1713	Vila Pouca de Aguiar	Vila Real	6,776439356	9	3,409482743	1,040836296

Table 5-Flood Shapefile

OBJECTID	DICO	Municipio	Distrito	MEAN_Slope	MEAN_Vegetation_Height	SUM_FlowAccumulation	MEAN_TWI	MEAN_Curvature
1	1109	Mafra	Lisboa	2,502335571	2,718715806	128019672	2,507914095	3,060913184
2	1106	Lisboa	Lisboa	3,872228246	3,441915776	70467383	2,422934628	3,940851621
3	1110	Oeiras	Lisboa	3,698968864	3,313192559	7476106	2,33262986	3,938196927
4	1115	Amadora	Lisboa	3,732117156	3,144993308	5584432	2,563484501	3,958933375
5	1015	Pombal	Leiria	5,600596048	2,074555262	221588143	2,231223158	2,830058031
6	1009	Leiria	Leiria	5,711636894	1,593047449	15904222	2,239299427	2,841257551
7	1421	Ourém	Santarém	5,810014129	2,114226692	40281149	2,182994911	2,819992959
8	0502	Castelo Branco	Castelo Branco	7,745810928	2,127583536	238366	2,070969605	2,934722234
9	0506	Oleiros	Castelo Branco	7,067573032	2,616957066	189547529	2,256604781	2,91978952
10	0508	Proença-a-Nova	Castelo Branco	6,931201189	2,672467058	180933349	2,499492588	2,927330515
11	0509	Sertã	Castelo Branco	7,315960943	2,647674658	98938614	2,390187004	2,913693965
12	0606	Góis	Coimbra	7,7756143	3,61266691	141842280	2,191962998	2,976528106
13	0607	Lousã	Coimbra	7,106705894	3,607213767	119554531	2,457394795	2,979304116
14	0609	Miranda do Corvo	Coimbra	7,885436182	3,693822165	13763423	2,212157911	2,977726924
15	1007	Castanheira de Pêra	Leiria	7,068745481	3,323612873	34257056	2,803891038	2,984214104
16	1008	Figueiró dos Vinhos	Leiria	7,144869123	3,298921444	8584053	2,921360017	2,979195725
17	1105	Cascais	Lisboa	5,044513002	2,410436482	108298807	2,194466782	2,893772699
18	1111	Sintra	Lisboa	5,394534189	2,904765655	215725838	2,154354121	2,901699496
19	1702	Boticas	Vila Real	7,989331404	3,644708061	16511677	2,220668537	2,860987533
20	1709	Ribeira de Pena	Vila Real	8,613708959	3,650463511	15849029	2,180269389	2,844186173
21	1713	Vila Pouca de Aguiar	Vila Real	6,776439356	3,409482743	92775572	2,278516724	2,869756043

4.2.1. Creation of the Raster hosted Tile

Only static project values were used to create the raster tile. Therefore, this visualization in Experience Builder is purely informative and for curiosity's sake, as it is possible to see how these variables alone influence the specific areas where LiDAR technology was used.

In ArcGIS Pro, the Contents pane (Figure 20) provides a comprehensive overview of all layers, tables, and other elements in the current project, allowing users to manage, organize, and symbolize their data efficiently. In this study, raster layers representing static variables such as slope, aspect, vegetation height, and vegetation density were first calculated individually. Subsequently, a weighted combination of these variables was performed using the Raster Calculator to generate composite risk layers. For fire risk, the weights were assigned as follows: Slope 0.25, Aspect 0.20, Vegetation Height 0.20, and Vegetation Density 0.35, summing to 100%. For flood risk, the weights were: Slope 0.20, Vegetation Height 0.10, Flow Accumulation 0.30, Topographic Wetness Index 0.30, and Curvature 0.10, also totaling 100%.

After calculating the weighted raster, the Contents pane was used to adjust the symbology of each layer. Risk classes were reclassified into categories from Low to extreme, and colours were customized to visually highlight areas of higher vulnerability. This approach allowed for clear visualization of spatial patterns of fire and flood risk across the study area and facilitated further analysis and sharing through ArcGIS Online (Figure 20).

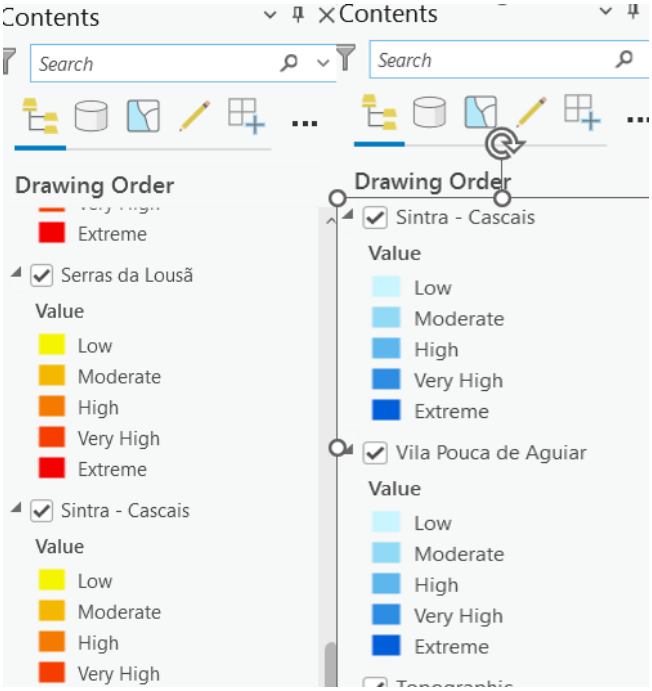

Figure 20-Contents pane -Fire and Flood Risk

Figures 21 and 22 illustrate the spatial distribution of fire and flood risk across the study area based on the weighted raster calculations. In these maps, areas with higher risk are clearly distinguishable from those with lower risk. For fire risk, regions with steeper slopes, denser vegetation, and south-facing aspects are highlighted as zones of higher vulnerability, whereas flatter or sparsely vegetated areas are classified as lower risk. Similarly, for flood risk, locations with high TWI values, greater flow accumulation, and concave terrain features are identified as more susceptible to flooding, while elevated or well-drained areas show lower vulnerability. These visualizations provide an intuitive understanding of the spatial patterns of environmental hazards and serve as a valuable tool for decision-making, planning, and resource allocation.

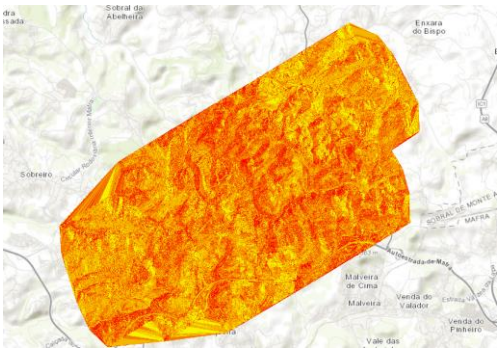

Figure 21-Raster Mafra: Wildfire Risk

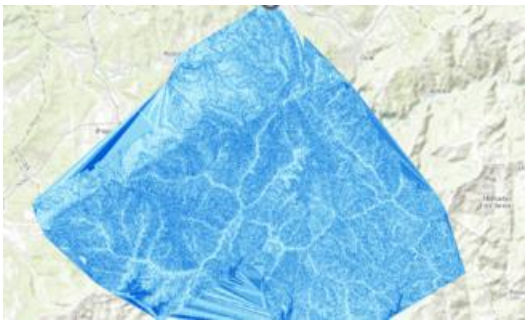

Figure 22-Raster Serras da Lousã- Flood Risk

4.3. Integration of Meteorological Data

The workflow for integrating meteorological data from IPMA Api´s is presented in figure 23:

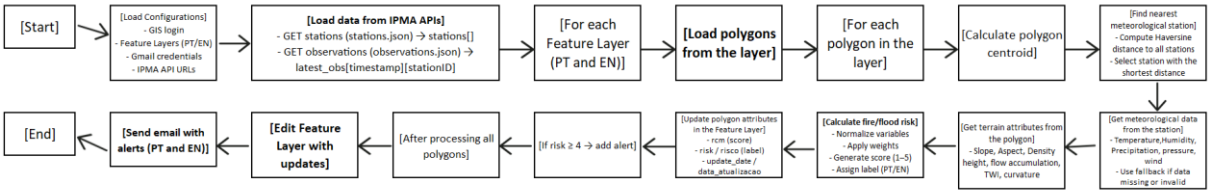

Figure 23-Workflow for integrating meteorological data from IPMA APIs with LiDAR-derived terrain attributes. The process includes system authentication, data retrieval from IPMA APIs (JSON), station assignment using Haversine distance, combination with terrain attributes, normalization and weighting of variables, calculation of fire and flood risk indices, and update of ArcGIS Online feature layers.

The integration of meteorological data into the risk calculation workflow was achieved using the IPMA public APIs. The process begins with the system configuration, which includes authentication with ArcGIS services, the identification of feature layers for the Portuguese and English versions of the application, and the specification of the API endpoints required for meteorological data retrieval. Once configured, the system retrieves both station metadata and the most recent observations in JSON format.

For each polygon within the feature layers, the algorithm computes its centroid and identifies the nearest meteorological station by calculating the Haversine distance to all available stations, ensuring that the most representative meteorological context is assigned. In cases where data are missing or invalid, a fallback mechanism is applied to guarantee continuity of the risk model.

After that, terrain attributes (such as slope, aspect, etc), are combined with the meteorological variables (temperature, humidity, etc) obtained from the nearest station [84].

For example, according to [85]in the municipality of Sintra, the centroid of the study polygon was calculated and the nearest meteorological station identified as ‘Colares/Sintra’ (ID = 1210747) at approximately 6 to 7 km from Sintra. From the IPMA API [40], the following observations were retrieved for 4 October 2025 at 08:00 UTC: temperature = 15.1 °C, humidity = 96%, wind speed = 32.4 km/h, and accumulated precipitation = 0.0 mm. These meteorological data were then combined with the LiDAR-derived terrain attributes of the polygon (mean slope = 5,39, aspect = 8, mean vegetation height = 2,9 m, mean density = 1,1) to calculate the corresponding fire and flood risk indices.

The combined dataset is then processed to calculate fire and flood risk indices. This involves the normalization of variables, the application of weighting factors based on literature. For fire risk, the weights applied to each variable are: Slope = 0.10, Aspect =0.05, Vegetation Height = 0.10, Vegetation Density = 0.10, Temperature = 0.25, Humidity = 0.20, Wind = 0.10, and Radiation = 0.10. For flood risk, the weights are: Slope = 0.10, Vegetation Height = 0.10, Flow Accumulation = 0.20, TWI = 0.15, Curvature = 0.10, Precipitation = 0.20, Pressure = 0.05, and Wind = 0.10.

The weighted variables are combined to generate a risk score on a scale from one to five for each polygon. Each polygon is updated with both a numerical score and a categorical risk label, available in Portuguese and English. If a polygon reaches a risk value above a predefined threshold (≥ 4), the system automatically issues email notifications containing alerts in both Portuguese and English

The updated risk information is subsequently written back to the ArcGIS Online feature layers and web map, ensuring that the web application always displays the most recent conditions.

This workflow guarantees the dynamic integration of static topographic information with real-time meteorological conditions, enabling the calculation and visualization of evolving fire and flood risk across the study areas.

4.4. Risk Index Calculation Algorithm

In Figures 24 and 25, screenshots of the weights used for the fire and flood risk calculations are presented.

```
WEIGHTS = {
    'slope': 0.1, 'aspect': 0.05, 'height': 0.1, 'density': 0.1,
    'temp': 0.25, 'hum': 0.2, 'vento': 0.1, 'rad': 0.1
}
```

Figure 24-Wild fire weights

```
WEIGHTS = {
    'slope': 0.1, 'height': 0.1, 'flowacc': 0.2,
    'twi': 0.15, 'curvature': 0.1,
    'prec': 0.2, 'pressao': 0.05, 'vento': 0.1
}
```

Figure 25-Flood Weights

It is important to note, that IPMA and other official sources do not provide detailed or fixed weights for individual variables such as slope, aspect, elevation, vegetation density, temperature, humidity, wind, and radiation. These weights are generally embedded within complex, integrated models and may vary depending on the context and application. In this work, the weights are assigned based on plausible values informed by previous experience, technical literature, and general knowledge of the relative influence of each variable on wildfire risk.

Studies such as [86], [87], [88]indicate that climatic factors, including temperature and humidity, have a stronger influence on wildfire risk, while topographic variables like slope, aspect, and the presence of infrastructure also play an important role. For flood risk, research by [89], [90], [91] highlights the importance of variables such as precipitation, land use, and slope in assessing susceptibility. Not only these studies, but the broader literature reviewed throughout this work, informed the selection of these weights, aiming to reflect the relative influence of each variable on the overall risk.

Meteorological factors like temperature and humidity are usually given higher weights, due to their direct and immediate effect on fire behaviour. Similarly, topographic, hydrological (including flow accumulation and TWI), and meteorological factors are integrators of the flood risk index. The concentration of water along the drainage network and the soil's tendency toward saturation are captured by hydrological variables. These markers are essential for locating regions at higher risk of flooding due to water accumulation. The most important meteorological factor is precipitation, which serves as the main cause of flooding incidents. This explains why TWI, precipitation, and flow accumulation are given higher weights.

4.5. Web Interface Development (ArcGIS Online Experience Builder)

To create the final web dashboard, an interactive web interface was developed using ArcGIS Online Experience Builder (Experience Builder is a tool within ArcGIS Online that allows users to design and deploy custom web applications and dashboards, integrating maps, data visualizations, and interactive widgets to support decision-making and data exploration.). This interface allows stakeholders to visualize, explore, and monitor fire and flood risk in real time, providing easy access to both numerical risk scores and qualitative risk categories.

The creation process involved three different projects: the feature layer, the story map, and the tile layer. The feature and tile layers were created using ArcGIS Pro and then shared on ArcGIS Online, while the story map was created directly in ArcGIS Online. The feature layers were then opened as a web map, and additional fields—named rcm, update_date, and risk—were added to display the results of the calculated risk indices. These fields are updated automatically using a Python script, which calculates the Risk Composite Metric (RCM), assigns qualitative risk categories, and records the time and date (US time zone). The script also enables email notifications whenever the risk of flooding or fire reaches or exceeds an RCM value of 4, ensuring that the interface provides up-to-date and actionable risk information.

Figures 26 and 27 illustrate examples of the automated email notifications generated by the system when the calculated RCM reaches or exceeds a threshold of 4. Figure 26 shows an email in English sent on September 15th at 17:58, reporting high risk levels for the following municipalities: Oeiras (RCM, Risk = Very High), Amadora (RCM = 4, Risk = Very High), and Castanheira de Pêra (RCM = 4, Risk = Very High). Figure 27 presents the corresponding email in Portuguese, containing the same information.

These figures demonstrate how the system communicates risk alerts in real time to stakeholders, ensuring that areas with elevated fire or flood risk are promptly identified and can be acted upon. The emails are automatically triggered by the Python script integrated with the ArcGIS Online feature layers, providing both the numerical RCM and the qualitative risk classification for each affected municipality.

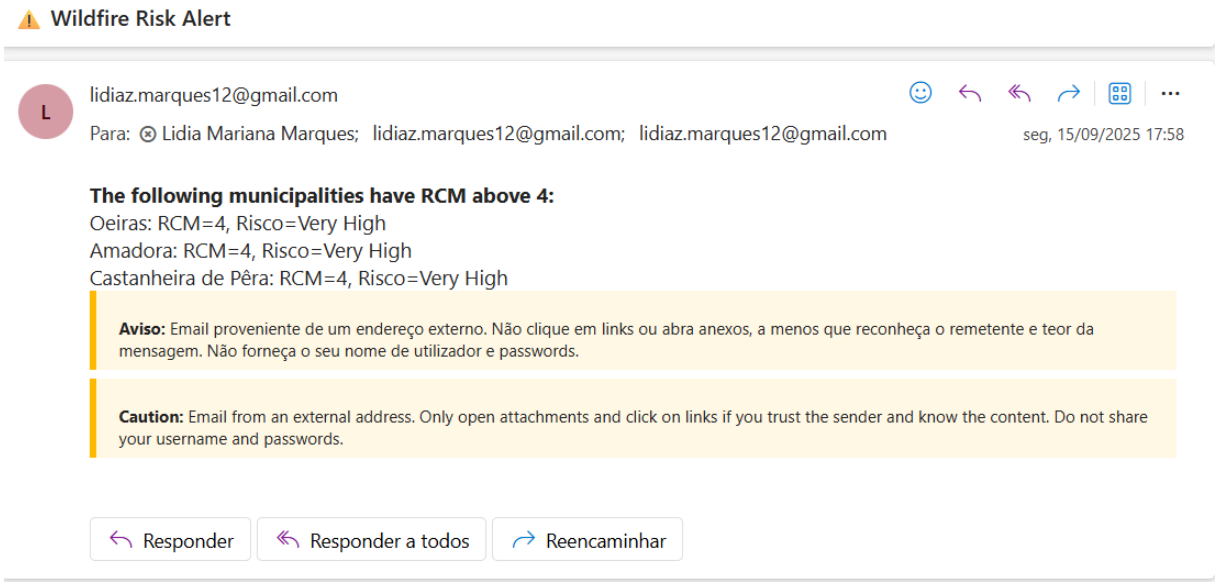

Figure 26-Communication of a risk alert via email (English Language)

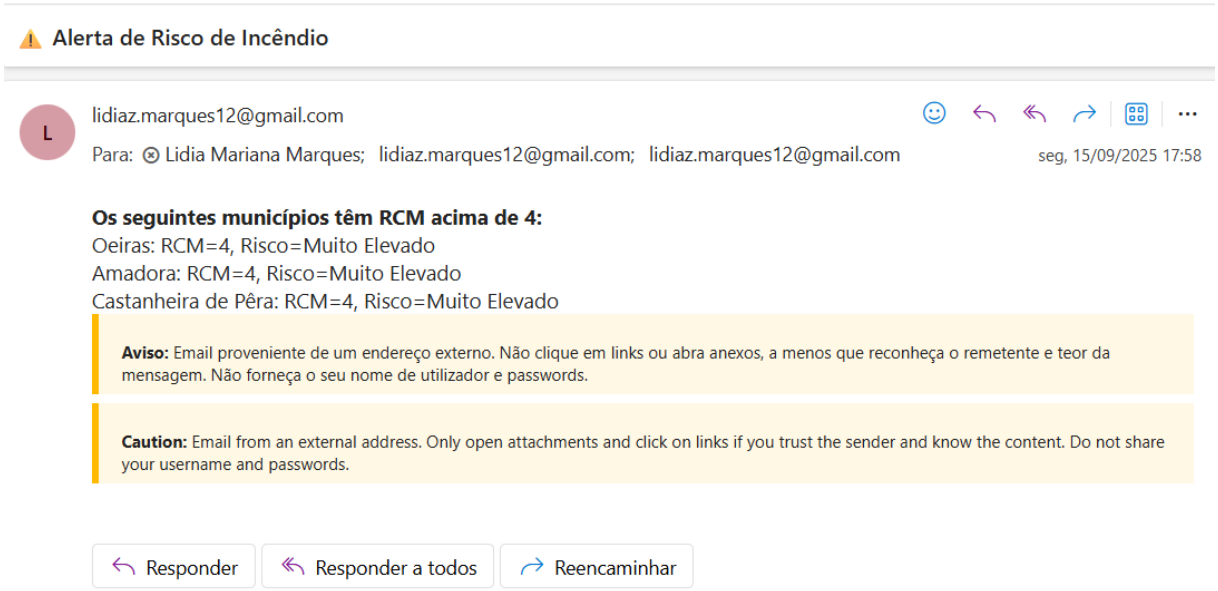

Figure 27-Communication of a risk alert via email (Portuguese Language)

Later, the feature layers and tile layers were saved as a web map so that we could later use the map widget in the Experience Builder dashboard.

After creating the web maps, it is time to create the Experience Builder, which we did by selecting the blank Fullscreen template. After that, we just had to use the Experience Builder features.

An Introduction was created, where we have an introduction, an explanation of the remote sensing data, and the fire and flood risk maps.

To conclude, at the web maps that contained the fire and flood risk feature layers, we have to change the pop-ups and styles to get the final "view," that is, for a more accurate view of fire and flood risk (change colours, choose, rcm, update_date and risk fields to appear in the table, the legend, the names of the municipalities, etc.). The same was done on the tile layer web map.

5. Results and Discussion

This chapter presents the outcomes of the integrated risk assessment system, demonstrating how LiDAR-derived variables, meteorological data, and the weighted risk index model combine to provide actionable insights on fire and flood risk across Portugal's study areas. The results highlight the effectiveness of the interactive web dashboard in visualizing risk, supporting decision-making, and communicating alerts to stakeholders.

5.1. Demonstration of the Application

The dashboard was developed using ArcGIS Online Experience Builder, with data layers and preprocessing performed in ArcGIS Pro. Feature and tile layers were created and published via ArcGIS Pro, while the story map was created directly in ArcGIS Online. Interactive functionality, such as polygon exploration, risk score visualization, and language switching (English/Portuguese), is implemented within Experience Builder, and real-time data updates are handled via Python scripts that integrate meteorological information from APIs.

The dashboard was created to offer an easy-to-use interface for examining environmental risk information from Portugal's 21 municipalities. It is organized into five primary sections, each of which has a distinct function in assisting the user in navigating the content.

The first section presents an explanation of the project Figure 28 and 29, explain the purpose and the reason why this app was created. The second section explains the data, including the characteristics and origins of it.
The third section, figure 30, approaches remote sensing map, which displays the seven regions covered by the LiDAR data. This map offers a real LiDAR perspective, since the risk of fire and flood are only calculated through the static data.

Fire and Flood Risk- Remote Sensing

What´s this project?

Lídia Marques
July 12, 2025

This project stems from a thesis proposal. The main objective would be to create an application that links the data from the ICNF's áGIL project with the IPMA's api's to describe the risk/probability of fire and flooding in that region at that time.

Figure 28-Experience Builder/Dashboard- Introduction in English

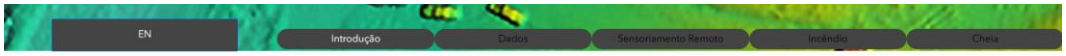

Incêndios e Cheias- Remote sensing

O que é este projeto?

Lídia Marques
July 12, 2025

Este projeto deriva de uma proposta de tese. O principal objetivo seria a criação de uma aplicação que relacionasse os dados do projeto áGIL do ICNF com as api´s do IPMA, para descrever o risco/probabilidade de incêndio e de cheia nesse momento nessa região.

Figure 29-Experience Builder/Dashboard-Introduction in Portuguese

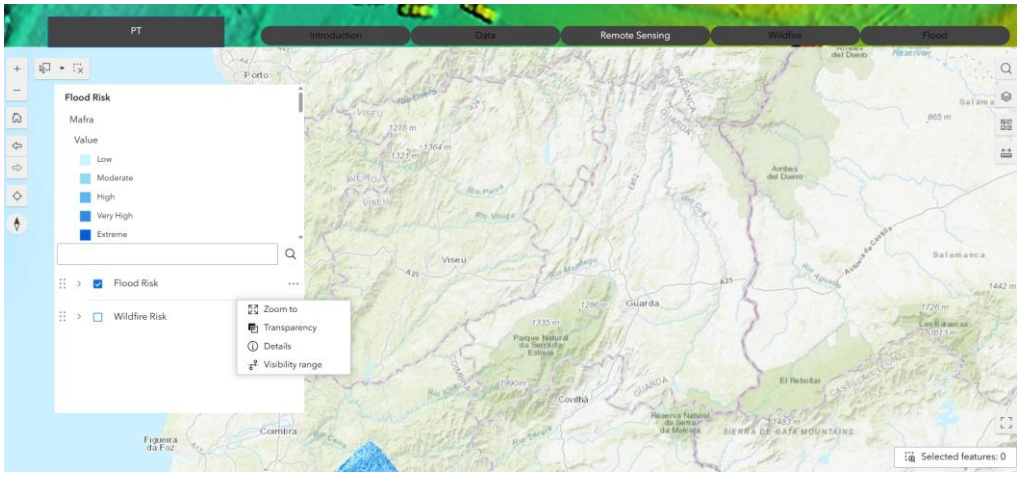

Figure 30-Experience Builder/Dashboard- Remote Sensing in English

The fourth and fifth sections, figure 31 and 32, focus on wildfire and flood risk, respectively. In these sections, the processed data are integrated with real-time meteorological information obtained via APIs. This allows the dashboard to display both static terrain-based indicators and dynamic weather conditions, highlighting areas of higher hazard across the study regions.

The maps include color-coded legends ranging from Low to Extreme risk levels, allowing users to quickly interpret hazard intensities across different regions.
At the top of the dashboard, users can navigate between the different sections of the application using a tabbed interface or a language selection button to switch between English and Portuguese. The tabs include Introduction, Data, Remote Sensing, Wildfire, and Flood, corresponding to the different components of the project.
In the fire risk tab, Vila Pouca de Aguiar was selected as an example, displaying a Risk Composite Metric (RCM) of 2, an update date of 16/09/2025 at 10:27 AM, and a qualitative risk label of Moderate. In the flood risk tab, Lisbon was selected, showing an RCM of 1, update date of 15/09/2025 at 7:07 PM, and a risk label of Low.

The interface allows users to toggle layers on and off, zoom into specific regions, and explore the following attributes for each municipality: RCM (Conjunctural and Meteorological Index), a numerical score reflecting the combined influence of multiple risk factors; update_date, which indicates the last time the risk data were calculated and updated; and risk, the qualitative risk category (Low, Moderate, High, Very High and Extreme) assigned based on the RCM value. This layered integration ensures that the dashboard functions as an interactive and informative tool for assessing and comparing risk across different regions of Portugal.

The update_date field comes from an extra hour than the Portuguese hour (During Daylight Saving Time) and the date format is MM/DD/YYYY instead of DD/MM/YYYY, because its serves Coordinated Universal Time (UTC).

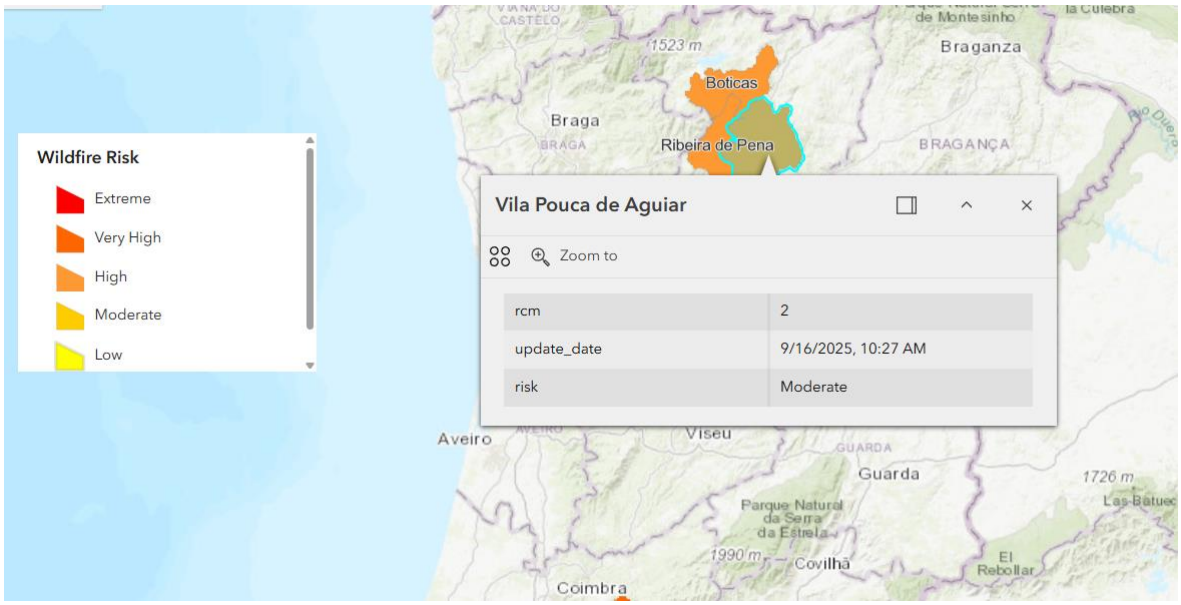

Figure 31-Experience Builder/Tab- Wildfire

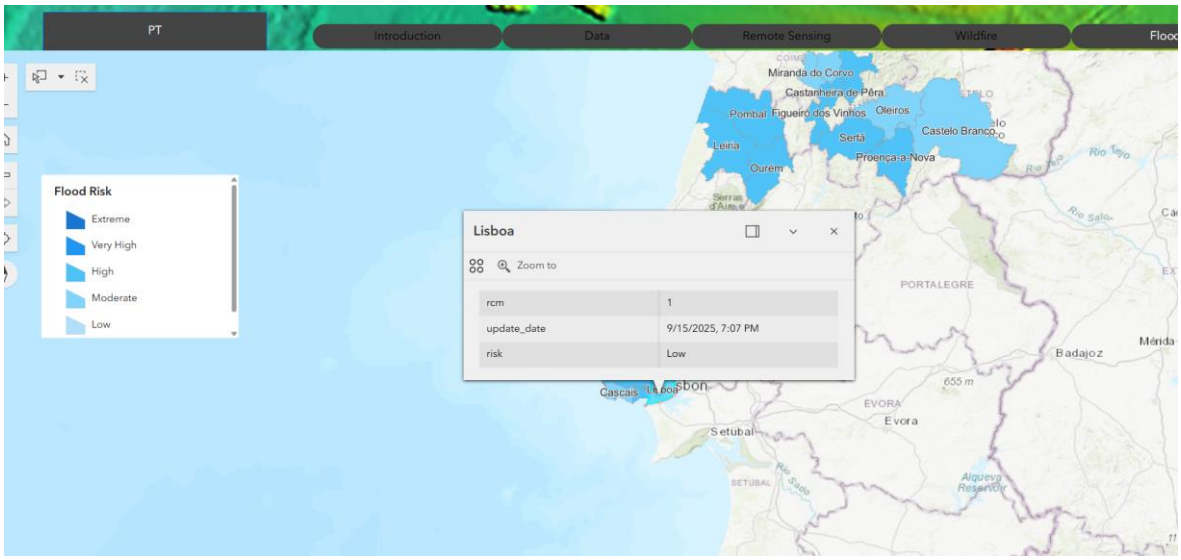

Figure 32-Experience Builder/Tab- Flood

5.2. Validation with Historical Events (e.g. IPMA fire risk data)

The validation of the proposed risk assessment system was conducted by comparing its outputs with the official RCM provided by IPMA, as well as through qualitative evaluation for flood risk. It is important to note that the IPMA does not publish the full formula for the RCM index; only general guidance is available, indicating that the index is derived from meteorological variables, fuel loads, and topographic factors. Their model has been calibrated empirically over decades for the Portuguese context.
In contrast, the methodology presented on this paper uses a simplified weighted scoring approach, where each variable is combined transparently to produce a daily risk index. As such, exact numerical agreement with IPMA's RCM is not expected.

To compare the wildfire risk index, the official IPMA API "Previsão do Risco de Incêndio até 2 dias, informação agregada por dia" was used [92]. The values obtained from the Python script in our application were then cross-checked with the RCM values from the IPMA API for the same day. The results of this comparison are summarized in Table 6, which lists the municipalities, their RCM values from the IPMA API, and the corresponding RCM values calculated by our system. As shown in the table, Lisbon, Oeiras, Amadora, Mafra, Sintra, and Cascais exhibit close alignment between the two sources, with RCM values of 2 or 3 (Figure 33).

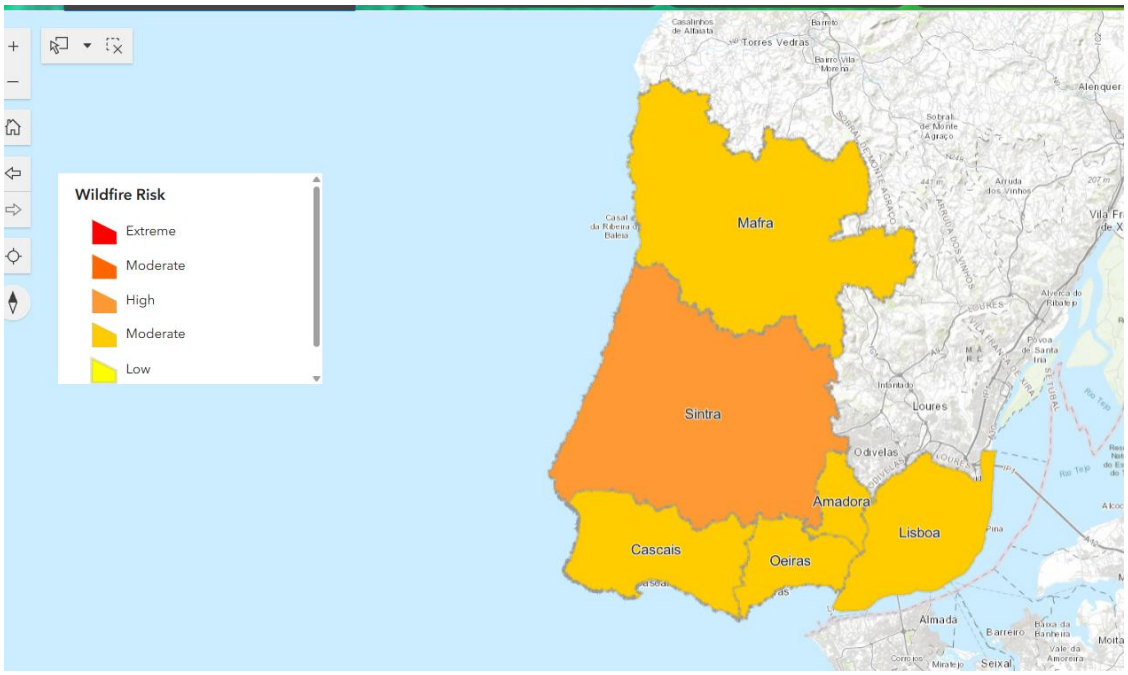

Figure 33-WIldifire index at 17/09/2025

Table 6-Risk Comparisons

	Script Values/Results		IPMA Values	
	Update_Date	rcm	date	Values
Lisboa	17/09/2025	2	17/09/2025	2
Oeiras	17/09/2025	2	17/09/2025	2
Amadora	17/09/2025	2	17/09/2025	2
Mafra	27/09/2025	2	27/09/2025	3
Sintra	17/09/2025	3	17/09/2025	3
Cascais	17/09/2025	2	17/09/2025	3

These are areas largely urban or semi-urban, with limited variability in vegetation cover and terrain. Consequently, even the simplified weighted model produces results that closely align with the official index. In contrast, municipalities with more complex topography or denser vegetation exhibit discrepancies, as the proposed system does not account for all factors used by IPMA, such as detailed fuel loads or soil moisture content [93], [94].

For flood risk, direct comparison with official indices is more challenging, as no standardized flood risk index exists from IPMA. Instead, validation was approached

qualitatively by comparing spatial patterns of the proposed index with known areas of susceptibility. The index incorporates terrain and hydrological variables which are recognized in the literature as key indicators of surface runoff and water accumulation.

In summary, the case study demonstrates that the proposed system captures the main patterns of both wildfire and flood risk, even if numerical values do not fully match official datasets. For wildfire, the alignment in urban areas confirms that the weighted scoring approach can reproduce known risk levels, while divergences in more complex terrains are justified by methodological differences. For flooding, the qualitative assessment shows that spatial patterns correspond to areas of high susceptibility.

5.3. Comparison with Existing Tools or Approaches

To place the developed model into context, it is relevant to compare it with the existing tools available that are being used in Portugal and Europe.
Table 7 summarizes a comparison between the proposed application system, the IPMA Fire Weather Index (FWI), and the Copernicus Emergency Management Service (EMS). This table highlights key differences in spatial and temporal resolution, variables considered, interactivity, and usability, illustrating how the proposed system addresses gaps in existing approaches.

Table 7- Risk Indexes Comparisons

Feature/Aspect	Web Application	IPMA FWI	Copernicus EMS
Spatial Resolution	Municipal / Local (high resolution, LiDAR-based)	Country-scale	Regional / Satellite-based
Temporal Resolution	Hourly, real-time updates via API	Daily	Near real-time (subject to satellite acquisition)
Variables Considered	Slope, aspect, vegetation height & density, temperature, humidity, wind, radiation, flow accumulation, TWI, curvature, precipitation, pressure	Meteorological variables influencing fire risk (temperature, wind, humidity, accumulated precipitation)	Satellite-derived hazard observations (fires, floods), terrain & land cover generalization
Interactivity / Usability	Web dashboard with interactive querying, email alerts, bilingual interface	Static maps (non-interactive)	Maps & reports for crisis management; limited local interactivity
Validation / Reference	Compared with historical RCM data from IPMA; qualitative evaluation for	Official national index	Qualitative comparison of spatial patterns; provides background for validation
Strengths	High-resolution, localized, integrated meteorological & terrain data, real-time	Official national index, empirically calibrated	Near real-time hazard monitoring at European scale
Limitations	Limited to seven regions of Agile project; simplified weighted model	Low spatial resolution; no interactivity	Large-scale focus, not tailored for municipal planning; temporal lags

The most widely applied source of fire danger information in Portugal is IPMA's daily published Fire Weather Index (FWI). The maps provide useful meteorological condition information that impacts fire danger; however, they are published at a country scale and lack detailed terrain or vegetation detail.
At the European level, Copernicus Emergency Management Service (EMS) provides near real time mapping and monitoring of natural hazards, including floods and wildfires [95].

Copernicus Emergency Management Service (CEMS) products are valuable as a robust external reference and for spatial validation due to their dependable high-resolution satellite and remote sensing data. Their maps of past and emergency events provide critical background for cross-tabulating emerging risk and hazard trends against new studies. Qualitative comparisons can be made through superimposition of established high-risk areas on CEMS wildfire and flood observations results. However, CEMS has its limitations, including temporal lags in the records, no continuous live updates, potential inconsistencies in spatial and temporal resolution from localized project-specific data (LiDAR, meteorological observations), and prioritization of rapid crisis response over daily operational forecast. Nevertheless, CEMS products serve as an indispensable standard of reference for cross-validation and qualitative comparison, lending strength to proposed methodologies that detect relevant spatial patterns of risk [95].

These services are broad-based and satellite-based on remote sensing, but their outputs are usually biased towards large-scale crisis management and lack the high spatial resolution needed at the municipal scale for planning. The Agile Project system addresses this gap by providing high-resolution data specific to each region in the seven areas covered, offering detailed spatial granularity and interactive features that aid in local-level decision-making.

6. Conclusions

This chapter presents the conclusions of this master's thesis and highlights how the research questions were addressed. It also outlines potential directions for future work and limitations.

6.1. Summary of Contributions

This dissertation has demonstrated the design and deployment of a prototype system integrating remote sensing and meteorological information to enable disaster risk estimation at the municipal level. The main contributions of this research are as follows, explicitly addressing the research questions:

"RQ1: Can we use a combination of remote sensing data, such as LiDAR data from the Agile Project, to accurately predict the risk of fire and flooding in the project area?"

In the first place, the research established the feasibility of combining terrain and vegetation parameters from LiDAR and real-time meteorological information from IPMA APIs. While most of the existing fire risk estimations in Portugal utilize meteorological indices exclusively, such as the Fire Weather Index (FWI), this research included descriptive spatial variables like slope, aspect, vegetation height, vegetation density, curvature, and topographic wetness index, thereby enriching the risk picture.

"RQ2: Can ArcGIS Experience Builder be used to integrate LiDAR data from the Agile Project with IPMA APIs through Python scripts?"

Second, the thesis presented an empirical solution to data merging and risk calculation. Using a literature-based idea weighted model, the system calculated dynamic fire and flood risk indexes that update in real time based on new meteorological data fetched. This provides a foundation for further research of more sophisticated predictive models. Third, the dissertation provided value through a working web application developed with ArcGIS Experience Builder. The application not only shows the merged datasets in real time but also has dashboards, support for two languages, and auto alerting features. This shows how municipal officials, and other parties could benefit from interactive and user-friendly tools for disaster risk monitoring.

Finally, the study also provided a proof of concept for the viability of applying the Agile Project LiDAR data to disaster management applications. Through the implementation of

the methodology to 21 municipalities, the research demonstrated how remote sensing large-scale projects could be transformed into decision-support applications that are both technically feasible and user-oriented.
Cumulatively, the research proves that the integration of high-resolution topography data and dynamic meteorological inputs can enhance local level risk analysis and produce an innovative idea for potential use in future disaster management.

Therefore, the research demonstrates that the integration of high-resolution topography data and dynamic meteorological inputs can enhance risk analysis at the local level, effectively answering the research questions and providing innovative approaches for future disaster management applications.

6.2. Limitations of the Study

Though the implemented system demonstrates the feasibility of fusing LiDAR-extracted terrain features and real-time weather conditions for disaster risk estimation, several limitations must be mentioned.
To begin with, the study was confined to the seven regions covered by the Agile Project. Although this provided it with a rational and practical scope, it inhibits the results from being generalized. The method would have to be tested at bigger and more heterogeneous geographical scales for its relevance to be established in different environmental and climatic conditions.
Expanding the system to cover the entire country would increase its utility and allow for national-level risk assessment and decision-making. To achieve this, additional LiDAR and meteorological data from other regions would need to be incorporated, and the model would require adaptation to account for regional differences in topography, vegetation, and climate. Challenges to this expansion include the availability and resolution of data, increased computational requirements, validation of the model across diverse regions, and maintaining an intuitive and interactive user interface.

Secondly, risk indices employed in this study were based on a simple weighted scoring technique. While this allows for straightforward incorporation of unlike variables, it fails to represent the complex, nonlinear processes that govern fire and flood behaviour. By contrast, established models such as the Fire Weather Index (FWI) are based on decades

of empirical validation, whereas the existing system remains a proof-of-concept awaiting refinement and calibration.

Third, the accuracy of the findings is subject to the accessibility and the quality of meteorological information at IPMA stations. In some cases, station coverage may be too sparse to capture local microclimatic conditions, especially in mountainous areas or areas with heterogeneous topography.

Finally, the project was built on the Esri platform, which includes ArcGIS Pro, ArcGIS Online, and Experience Builder. While these platforms provide an extensive environment for development it is not open source such as QGIS, so their use is limited to people who have access to them.

Despite these limitations, the contribution makes a productive foundation for subsequent research and development. The system establishes a conceptual and technical framework that can be progressively enhanced through increased validation, incorporation of advanced modelling techniques, and adaptation to diverse technological environments.

6.3. Recommendations and Future Work

Since these limitations are recognized, some directions for future research and development are proposed.

First, the Agile Project LiDAR dataset covered just a limited portion of Portuguese territory. The methodology should cover the rest of the territory, beyond the seven regions covered by the Agile Project, in order to test its scalability and robustness across different geographic and climatic contexts. Access to newer high-resolution data at a national scale would significantly improve the accuracy of risk modelling and enable fair comparison of regions.

Second, the weighted scoring technique used in this dissertation could be evolved into advanced modelling systems. Machine learning or statistical methods could be used to derive nonlinear relationships between terrain, vegetation, and meteorological data. These methodologies can also facilitate ongoing model calibration via historical fire and flood events, leading to better predictive performance over the years.

Finally, cooperation with environmental agencies, municipalities, and civil protection authorities would be essential to evaluate the system in real field conditions. Pilot

deployments in real operating environments would have the effect of providing usability feedback, data requirements, and decision-making effectiveness, ensuring that the tool is refined to become a useful decision-making support system rather than an academic exercise/tool.

In summary, future actions need to focus on creating more comprehensive coverage of data, support modelling approaches, raise technical availability, and enhance institutional collaboration. This would play a very powerful role in improving disaster risk management in Portugal and elsewhere through remote sensing and geospatial technology.

References

[1] I. Castro-Melgar, T. Falaras, E. Basiou, and I. Parcharidis, “Assessment of the October 2024 Cut-Off Low Event Floods Impact in Valencia (Spain) with Satellite and Geospatial Data,” *Remote Sens (Basel)*, vol. 17, no. 13, Jul. 2025, doi: 10.3390/rs17132145.

[2] F. Yilgan, N. Yildiz, and T. Dogan, “Assessing the environmental impacts of the Capilla del Monte wildfire in Punilla Valley of Argentina using Landsat-9 and Sentinel-5P,” *Environ Monit Assess*, vol. 197, no. 8, Aug. 2025, doi: 10.1007/s10661-025-14374-y.

[3] I. O. Abu and C. C. Ibebuchi, “Risk Assessment of the 2022 Nigerian Flood Event Using Remote Sensing Products and Climate Data,” *Remote Sens (Basel)*, vol. 17, no. 11, Jun. 2025, doi: 10.3390/rs17111814.

[4] D. Sykas, D. Zografakis, K. Demestichas, C. Costopoulou, and P. Kosmidis, “EO4WildFires: An Earth Observation multi-sensor, time-series machine-learning-ready benchmark dataset for wildfire impact prediction”, doi: 10.5281/zenodo.7762564.

[5] Auld Heather, “Disaster risk reduction under current and changing climate Title conditions.” [Online]. Available: www.em-dat.net

[6] I. L. Coimbra, J. Mann, J. M. L. M. Palma, and V. T. P. Batista, “Exploring dual-lidar mean and turbulence measurements over Perdigão’s complex terrain,” *Atmos Meas Tech*, vol. 18, no. 1, pp. 287–303, Jan. 2025, doi: 10.5194/amt-18-287-2025.

[7] G. K. Wedajo, “LiDAR DEM Data for Flood Mapping and Assessment; Opportunities and Challenges: A Review,” *Journal of Remote Sensing & GIS*, vol. 06, no. 04, 2017, doi: 10.4172/2469-4134.1000211.

[8] L. Magnini, D. Pozzi-Escot, J. Oshiro, R. Angeles, M. I. P. Apa, and G. Ventura, “Effects of the Architectural Layout of the Sanctuary of Pachacamac (2nd–16th Century CE, Peru) on the Exposure to Rain, Wind, and Solar Radiation from the Morphometric Analysis of Digital Surface Models,” *Remote Sens (Basel)*, vol. 16, no. 11, Jun. 2024, doi: 10.3390/rs16111848.

[9] B. D. Song, S. Jun, and S. Lee, “Integrated System Design for Post-Disaster Management: Multi-Facility, Multi-Period, and Bi-Objective Optimization Approach,” *Systems*, vol. 12, no. 3, Mar. 2024, doi: 10.3390/systems12030069.

[10] T. Çömez Ikican, G. Şahin Bayindir, Y. Engin, and E. Albal, “Disaster preparedness perceptions and psychological first-aid competencies of psychiatric nurses,” *Int Nurs Rev*, vol. 72, no. 2, Jun. 2025, doi: 10.1111/inr.13036.

[11] S. Sazlin *et al.*, “Five Phases Cycles in Emergency Preparedness and Response Plan (EPRP) s An Emergency Management For Campus Environment,” 2024. [Online]. Available: http://www.akademiabaru.com/submit/index.php/artim/index

[12] N. Göktepe, D. Güneş, P. B. Güler, G. Z. Aydin, and M. Amarat, “The mediating role of disaster response self-efficacy in the effect of disaster anxiety on the willingness to work in disasters among the nurses,” *BMC Nurs*, vol. 24, no. 1, Dec. 2025, doi: 10.1186/s12912-025-03564-1.

[13] H. A. S. Al Mekhlefi and J. Liu, “Critical factors influencing post-disaster reconstruction: A quantitative analysis of Yemen’s recovery challenges,” *Ain*

Shams Engineering Journal, vol. 16, no. 9, Sep. 2025, doi: 10.1016/j.asej.2025.103538.
[14] L. Pearce, "Disaster management and community planning, and public participation: How to achieve sustainable hazard mitigation," *Natural Hazards*, vol. 28, no. 2–3, pp. 211–228, Mar. 2003, doi: 10.1023/A:1022917721797.
[15] V. Leone, M. Elia, R. Lovreglio, F. Correia, and F. Tedim, "The 2017 Extreme Wildfires Events in Portugal through the Perceptions of Volunteer and Professional Firefighters," *Fire*, vol. 6, no. 4, Apr. 2023, doi: 10.3390/fire6040133.
[16] Gill Joanna, "Portugal fights wildfires with new tactics as heatwaves raise risk," 15 july 2022. Accessed: Oct. 04, 2025. [Online]. Available: https://www.preventionweb.net/news/portugal-fights-wildfires-new-tactics-heatwaves-raise-risk
[17] Mayers Lily, "THE OPEN WOUNDS OF PEDRÓGÃO GRANDE THE AFTERMATH OF ONE OF PORTUGAL'S DEADLIEST MEGA FIRES." Accessed: Oct. 04, 2025. [Online]. Available: https://www.iawfonline.org/article/the-open-wounds-of-pedrogao-grande/
[18] Duarte Dina, "Burocracia e falta de coordenação ainda prejudica vítimas dos fogos de Pedrogão em 2017." Accessed: Oct. 04, 2025. [Online]. Available: https://www.rtp.pt/noticias/pais/burocracia-e-falta-de-coordenacao-ainda-prejudica-vitimas-dos-fogos-de-pedrogao-em-2017_a1678312
[19] "Estabelece medidas de apoio às vítimas dos incêndios florestais ocorridos em Portugal continental entre 17 e 24 de junho de 2017 e 15 e 16 de outubro de 2017, bem como medidas urgentes de reforço da prevenção e combate a incêndios florestais." Accessed: Oct. 04, 2025. [Online]. Available: https://diariodarepublica.pt/dr/legislacao-consolidada/lei/2017-114834172
[20] Z. Li, K. Kosová, Z. Kaixing, and Z. Ding, "Evaluation of important phenotypic parameters of tea plantations using multi-source remote sensing data."
[21] L. Bian, A. M. Melesse, A. S. Leon, V. Verma, and Z. Yin, "A deterministic topographic wetland index based on lidar-derived dem for delineating open-water wetlands," *Water (Switzerland)*, vol. 13, no. 18, Sep. 2021, doi: 10.3390/w13182487.
[22] M. Zeybek, "Inlier Point Preservation in Outlier Points Removed from the ALS Point Cloud," *Journal of the Indian Society of Remote Sensing*, vol. 49, no. 10, pp. 2347–2363, Oct. 2021, doi: 10.1007/s12524-021-01397-4.
[23] T. R. Cody and S. L. Anderson, "LiDAR predictive modeling of Pacific Northwest mound sites: A study of Willamette Valley Kalapuya Mounds, Oregon (USA)," *J Archaeol Sci Rep*, vol. 38, Aug. 2021, doi: 10.1016/j.jasrep.2021.103008.
[24] B. E. Aissou, A. B. Aissa, A. Dairi, F. Harrou, A. Wichmann, and M. Kada, "Building Roof Superstructures Classification from Imbalanced and Low Density Airborne LiDAR Point Cloud," *IEEE Sens J*, vol. 21, no. 13, pp. 14960–14976, Jul. 2021, doi: 10.1109/JSEN.2021.3073535.
[25] Z. Kuang, D. Liu, D. Wu, Z. Wang, C. Li, and Q. Deng, "Parameter Optimization and Development of Mini Infrared Lidar for Atmospheric Three-Dimensional Detection," *Sensors*, vol. 23, no. 2, Jan. 2023, doi: 10.3390/s23020892.
[26] H. Zhong *et al.*, "Identification of tree species based on the fusion of UAV hyperspectral image and LiDAR data in a coniferous and broad-leaved mixed forest in Northeast China," *Front Plant Sci*, vol. 13, Sep. 2022, doi: 10.3389/fpls.2022.964769.

[27] Galang wenyville, Tabañag Ian, and Loretero Michael, “Approach on Biomass Energy Potential Estimation of Sugarcane Residues in Medellin. Cebu”.
[28] A. Monterroso-Checa, J. C. Moreno-Escribano, M. Gasparini, J. A. Conejo-Moreno, and J. L. Domínguez-Jiménez, “Revealing archaeological sites under mediterranean forest canopy using LiDAR: El viandar castle (husum) in El Hoyo (Belmez-Córdoba, Spain),” *Drones*, vol. 5, no. 3, Sep. 2021, doi: 10.3390/drones5030072.
[29] P. Gili, M. Civera, R. Roy, and C. Surace, “An unmanned lighter-than-air platform for large scale land monitoring,” *Remote Sens (Basel)*, vol. 13, no. 13, Jul. 2021, doi: 10.3390/rs13132523.
[30] A. N. Nunes, A. Figueiredo, C. Pinto, and L. Lourenço, “Assessing Wildfire Hazard in the Wildland–Urban Interfaces (WUIs) of Central Portugal,” *Forests*, vol. 14, no. 6, Jun. 2023, doi: 10.3390/f14061106.
[31] J. M. Fernández-Guisuraga and P. M. Fernandes, “Using Pre-Fire High Point Cloud Density LiDAR Data to Predict Fire Severity in Central Portugal,” *Remote Sens (Basel)*, vol. 15, no. 3, Feb. 2023, doi: 10.3390/rs15030768.
[32] T. Ermitão, P. Páscoa, I. Trigo, C. Alonso, and C. Gouveia, “Mapping the Most Susceptible Regions to Fire in Portugal,” *Fire*, vol. 6, no. 7, Jul. 2023, doi: 10.3390/fire6070254.
[33] O. Martin-Ducup *et al.*, “Unlocking the potential of Airborne LiDAR for direct assessment of fuel bulk density and load distributions for wildfire hazard mapping,” *Agric For Meteorol*, vol. 362, Mar. 2025, doi: 10.1016/j.agrformet.2024.110341.
[34] IPMA, “Plano de atividade do IPMA para 2025,” 2025.
[35] A. K. Das and S. Ghosh, “Development and Evaluation of a User-Friendly and Lightweight Weather Map Application: Enhancing Access to Real-Time Meteorological Data,” in *2023 7th International Conference on Electronics, Materials Engineering and Nano-Technology, IEMENTech 2023*, Institute of Electrical and Electronics Engineers Inc., 2023. doi: 10.1109/IEMENTech60402.2023.10423443.
[36] Documentation ESRI, “Arcgis Gis software”.
[37] C. Cocq, O. Cenk Demiroglu, U. Lindgren, L. Granstedt, and E. Lindgren, “A web experience exploring spatio–linguistic data: the case of place-making signs in Northern Sweden,” *J Maps*, vol. 20, no. 1, 2024, doi: 10.1080/17445647.2024.2370310.
[38] X. De Lamo, “INTRODUCTION TO QGIS,” 2017.
[39] ICNF, “Projeto áGIL - Dados LiDAR.” Accessed: Oct. 04, 2025. [Online]. Available: https://geocatalogo.icnf.pt/geovisualizador/agil.html
[40] IPMA, “Observação Meteorológica de Estações (dados horários, últimas 24 horas).” Accessed: Oct. 04, 2025. [Online]. Available: https://api.ipma.pt/open-data/observation/meteorology/stations/observations.json
[41] IPMA, “IPMA API -Interface de Programação de Aplicações do IPMA.” Accessed: Oct. 04, 2025. [Online]. Available: https://api.ipma.pt/
[42] Documentation ESRI, “LAS Dataset To Raster (Conversion).” [Online]. Available: https://pro.arcgis.com/en/pro-app/latest/tool-reference/conversion/las-dataset-to-raster.htm
[43] Documentation ESRI, “LAS To Multipoint (3D Analyst).” Accessed: Oct. 04, 2025. [Online]. Available: https://pro.arcgis.com/en/pro-app/3.4/tool-reference/3d-analyst/las-to-multipoint.htm
[44] Documentation ESRI, “Point Density (Spatial Analyst).”

[45] Documentation ESRI, “Generate a DTM using ArcGIS Reality for ArcGIS Pro.” [Online]. Available: https://pro.arcgis.com/en/pro-app/latest/help/data/imagery/generate-a-dtm-using-arcgis-reality.htm
[46] Documentation ESRI, “Generate a DSM using ArcGIS Reality for ArcGIS Pro.” Accessed: Oct. 04, 2025. [Online]. Available: https://pro.arcgis.com/en/pro-app/latest/help/data/imagery/generate-a-dsm-using-arcgis-reality.htm
[47] Gimond Manuel, “Intro to GIS and Spatial Analysis.” Accessed: Oct. 04, 2025. [Online]. Available: https://mgimond.github.io/Spatial/
[48] “Analyzing Spatial Patterns.” Accessed: Oct. 04, 2025. [Online]. Available: https://mgimond.github.io/Spatial/chp11_0.html#density-based-analysis
[49] Documentation ESRI, “LAS dataset statistics.” Accessed: Oct. 04, 2025. [Online]. Available: https://pro.arcgis.com/en/pro-app/latest/help/data/las-dataset/work-with-las-dataset-statistics.htm
[50] “Lidar-Base-Specification-version-2-1”.
[51] Documentation ESRI, “LAS Dataset To Raster function.” Accessed: Oct. 04, 2025. [Online]. Available: https://pro.arcgis.com/en/pro-app/latest/help/analysis/raster-functions/las-dataset-to-raster-function.htm
[52] P. F. Evangelista and D. Beskow, “Geospatial Point Density,” 2018.
[53] U. BALTACI and F. YILDIRIM, “Effect of Slope on the Analysis of Forest Fire Risk,” *Hacettepe Journal of Biology and Chemistry*, vol. 48, no. 4, pp. 373–379, Jul. 2020, doi: 10.15671/hjbc.753080.
[54] K. C. Ryan, “FOREST FIRE HAZARD AND RISK,” 1976.
[55] M. J. Schroeder, “Fire_Weather,” 1970.
[56] T. Beer, “THE INTERACTION OF WIND AND FIRE (Review Article),” 1990.
[57] M. Ghodrat, F. Shakeriaski, D. J. Nelson, and A. Simeoni, “Existing Improvements in Simulation of Fire–Wind Interaction and Its Effects on Structures,” Jun. 01, 2021, *MDPI*. doi: 10.3390/FIRE4020027.
[58] A. Purwanto, D. Andrasmoro, and Eviliyanto, “Use of HAND Model for Estimating Flood-Prone in Serawai Basins Base on Remote Sensing and Sistem Information Geography,” *Indonesian Journal of Geography*, vol. 56, no. 3, pp. 436–445, 2024, doi: 10.22146/ijg.89225.
[59] A. Motevalli and M. Vafakhah, “Flood hazard mapping using synthesis hydraulic and geomorphic properties at watershed scale,” *Stochastic Environmental Research and Risk Assessment*, vol. 30, no. 7, pp. 1889–1900, Oct. 2016, doi: 10.1007/s00477-016-1305-8.
[60] N. S. Cunha, M. R. Magalhães, T. Domingos, M. M. Abreu, and C. Küpfer, “The land morphology approach to flood risk mapping: An application to Portugal,” *J Environ Manage*, vol. 193, pp. 172–187, May 2017, doi: 10.1016/j.jenvman.2017.01.077.
[61] G. Toosi, “Influence of Vegetation in The Flood Drainage Ditch,” *Journal of Civil Engineering Researchers*, no. 4, pp. 16–21, 2017, doi: 10.52547/JCER.5.4.16.
[62] H. Tabari, “Climate change impact on flood and extreme precipitation increases with water availability,” *Sci Rep*, vol. 10, no. 1, Dec. 2020, doi: 10.1038/s41598-020-70816-2.
[63] P. A. Pirazzoli, “Surges, atmospheric pressure and wind change and flooding probability on the Atlantic coast of France,” 2000.
[64] Documentation ESRI, “20034: Your web layer will use the WGS 1984 Web Mercator (Auxiliary Sphere) coordinate system.” Accessed: Oct. 04, 2025. [Online]. Available: https://pro.arcgis.com/en/pro-

app/latest/help/sharing/analyzer-warning-messages/20034-your-web-layer-will-use-the-wgs-1984-web-mercator-coordinate-system.htm
[65] Documentation ESRI, "Slope (Spatial Analyst)." Accessed: Oct. 04, 2025. [Online]. Available: https://pro.arcgis.com/en/pro-app/latest/tool-reference/spatial-analyst/slope.htm
[66] Documentation ESRI, "Aspect (Spatial Analyst)." Accessed: Oct. 04, 2025. [Online]. Available: https://pro.arcgis.com/en/pro-app/3.4/tool-reference/spatial-analyst/aspect.htm
[67] Documentation ESRI, "Curvature (Spatial Analyst)." Accessed: Oct. 04, 2025. [Online]. Available: https://pro.arcgis.com/en/pro-app/3.4/tool-reference/spatial-analyst/curvature.htm
[68] Documentation ESRI, "Raster Calculator (Spatial Analyst)." Accessed: Oct. 04, 2025. [Online]. Available: https://pro.arcgis.com/en/pro-app/3.3/tool-reference/spatial-analyst/raster-calculator.htm
[69] Documentation ESRI, "Fill (Spatial Analyst)." Accessed: Oct. 04, 2025. [Online]. Available: https://pro.arcgis.com/en/pro-app/latest/tool-reference/spatial-analyst/fill.htm
[70] Documentation ESRI, "Flow Direction (Spatial Analyst)." Accessed: Oct. 04, 2025. [Online]. Available: https://pro.arcgis.com/en/pro-app/latest/tool-reference/spatial-analyst/flow-direction.htm
[71] Documentation ESRI, "Flow Accumulation (Spatial Analyst)." Accessed: Oct. 04, 2025. [Online]. Available: https://pro.arcgis.com/en/pro-app/latest/tool-reference/spatial-analyst/flow-accumulation.htm
[72] R. Sørensen, U. Zinko, and J. Seibert, "On the calculation of the topographic wetness index: Evaluation of different methods based on field observations," *Hydrol Earth Syst Sci*, vol. 10, no. 1, pp. 101–112, 2006, doi: 10.5194/hess-10-101-2006.
[73] D. G. Tarboton, "A new method for the determination of flow directions and upslope areas in grid digital elevation models," *Water Resour Res*, vol. 33, no. 2, pp. 309–319, 1997, doi: 10.1029/96WR03137.
[74] "How to convert Degrees to Radians." Accessed: Oct. 04, 2025. [Online]. Available: https://polytechnicmaster.blogspot.com/2018/06/how-to-convert-degrees-to-radians.html
[75] "Carta Administrativa Oficial de Portugal - CAOP 2023." Accessed: Oct. 04, 2025. [Online]. Available: https://www.dgterritorio.gov.pt/Carta-Administrativa-Oficial-de-Portugal-CAOP-2023
[76] Documntation ESRI, "Reclassify (Spatial Analyst)." Accessed: Oct. 04, 2025. [Online]. Available: https://pro.arcgis.com/en/pro-app/latest/tool-reference/spatial-analyst/reclassify.htm
[77] G. Singh Editors, "Geotechnologies and the Environment Geospatial Technologies in Land Resources Mapping, Monitoring and Management." [Online]. Available: http://www.springer.com/series/8088
[78] Documentation ESRI, "How zonal statistics tools work." Accessed: Oct. 04, 2025. [Online]. Available: https://pro.arcgis.com/en/pro-app/latest/tool-reference/spatial-analyst/how-zonal-statistics-works.htm
[79] Documentation ESRI, "Zonal Statistics as Table (Spatial Analyst)." [Online]. Available: https://pro.arcgis.com/en/pro-app/latest/tool-reference/spatial-analyst/zonal-statistics-as-table.htm

[80] “Zonal Statistics-Overview.” Accessed: Oct. 04, 2025. [Online]. Available: https://knowledge.deck.no/geography/geographic-information-systems-gis/spatial-analysis/zonal-statistics
[81] P. A. Burrough and R. A. Mcdonnell, “Principles of Geographical Information Systems,” 1998.
[82] Documentation ESRI, “How zonal statistics Work.” Accessed: Oct. 04, 2025. [Online]. Available: https://desktop.arcgis.com/en/arcmap/latest/tools/spatial-analyst-toolbox/how-zonal-statistics-works.htm
[83] Documentation ESRI, “Merge (Data Management).” Accessed: Oct. 04, 2025. [Online]. Available: https://pro.arcgis.com/en/pro-app/3.4/tool-reference/data-management/merge.htm
[84] “Haversine formula in python (bearing and distance between two gps points).” Accessed: Oct. 04, 2025. [Online]. Available: https://stackoverflow.com/questions/4913349/haversine-formula-in-python-bearing-and-distance-between-two-gps-points
[85] IPMA, “Lista de identificadores das estações meteorológicas.” Accessed: Oct. 04, 2025. [Online]. Available: https://api.ipma.pt/open-data/observation/meteorology/stations/stations.json
[86] G. Salavati, E. Saniei, E. Ghaderpour, and Q. K. Hassan, “Wildfire Risk Forecasting Using Weights of Evidence and Statistical Index Models,” *Sustainability (Switzerland)*, vol. 14, no. 7, Apr. 2022, doi: 10.3390/su14073881.
[87] J. H. Scott, M. P. Thompson, and D. E. Calkin, “A Wildfire Risk Assessment Framework for Land and Resource Management,” 2013. [Online]. Available: http://www.fs.fed.us/rmrs
[88] A. A. Gerdzheva, “A COMPARATIVE ANALYSIS OF DIFFERENT WILDFIRE RISK ASSESSMENT MODELS (A CASE STUDY FOR SMOLYAN DISTRICT, BULGARIA),” 2014. [Online]. Available: https://www.uni-sofia.bg/index.php/eng
[89] A. Mohamed Elmoustafa, “Weighted normalized risk factor for floods risk assessment,” *Ain Shams Engineering Journal*, vol. 3, no. 4, pp. 327–332, 2012, doi: 10.1016/j.asej.2012.04.001.
[90] A. Maranzoni, M. D’Oria, and C. Rizzo, “Quantitative flood hazard assessment methods: A review,” Mar. 01, 2023, *John Wiley and Sons Inc*. doi: 10.1111/jfr3.12855.
[91] N. Tabasi, M. Fereshtehpour, and B. Roghani, “A review of flood risk assessment frameworks and the development of hierarchical structures for risk components,” *Discover Water*, vol. 5, no. 1, Feb. 2025, doi: 10.1007/s43832-025-00193-2.
[92] IPMA, “Previsão do Risco de Incêndio até 2 dias, informação agregada por dia (day 0).” Accessed: Oct. 04, 2025. [Online]. Available: https://api.ipma.pt/open-data/forecast/meteorology/rcm/rcm-d0.json
[93] F. Schug *et al.*, “The global wildland–urban interface,” *Nature*, vol. 621, no. 7977, pp. 94–99, Sep. 2023, doi: 10.1038/s41586-023-06320-0.
[94] N. A. Povak, P. F. Hessburg, and R. B. Salter, “Evidence for scale-dependent topographic controls on wildfire spread,” *Ecosphere*, vol. 9, no. 10, Oct. 2018, doi: 10.1002/ecs2.2443.
[95] Copernicus, “Copernicus Emergency Management Service.” Accessed: Oct. 04, 2025. [Online]. Available: https://emergency.copernicus.eu/

Appendices

Web Application

The interactive dashboard developed in ArcGIS Experience Builder can be accessed at the following link:

https://experience.arcgis.com/experience/8c9454bf5d6345b0bffd0352617ba727/page/Introdu%C3%A7%C3%A3o?draft=true